

A COMPREHENSIVE GRAPH POOLING BENCHMARK: EFFECTIVENESS, ROBUSTNESS AND GENERALIZABILITY

Anonymous authors

Paper under double-blind review

ABSTRACT

Graph pooling has gained attention for its ability to obtain effective node and graph representations for various downstream tasks. Despite the recent surge in graph pooling approaches, there is a lack of standardized experimental settings and fair benchmarks to evaluate their performance. To address this issue, we have constructed a comprehensive benchmark that includes 17 graph pooling methods and 28 different graph datasets. This benchmark systematically assesses the performance of graph pooling methods in three dimensions, i.e., effectiveness, robustness, and generalizability. We first evaluate the performance of these graph pooling approaches across different tasks including graph classification, graph regression and node classification. Then, we investigate their performance under potential noise attacks and out-of-distribution shifts in real-world scenarios. We also involve detailed efficiency analysis, backbone analysis, parameter analysis and visualization to provide more evidence. Extensive experiments validate the strong capability and applicability of graph pooling approaches in various scenarios, which can provide valuable insights and guidance for deep geometric learning research. The source code of our benchmark is available at https://anonymous.4open.science/r/Graph_Pooling_Benchmark-8EDD.

1 INTRODUCTION

Recently, graph neural networks (GNNs) have garnered significant attention with extensive benchmarks (Tan et al., 2023; Li et al., 2024; Hu et al., 2020a) due to their remarkable ability to process graph-structured data across various domains including social networks (Wu et al., 2020a; Yang et al., 2021; Zhang et al., 2022), rumor detection (Bian et al., 2020; Zhang et al., 2023), biological networks (Wu et al., 2018; Choi et al., 2020), recommender systems (Ma et al., 2020a) and community detection (Alsentzer et al., 2020; Sun et al., 2022). Graph pooling approaches play a crucial role in GNNs by enabling the hierarchical reduction of graph representations, which is essential for capturing multi-scale structures and long-range dependencies (Liu et al., 2022a; Wu et al., 2022b; Dwivedi et al., 2023). They can preserve crucial topological semantics and relationships, which have shown effective for tasks including graph classification, node clustering, and graph generation (Liu et al., 2022a; 2020; Grattarola et al., 2022a; Li et al., 2024). In addition, by aggregating nodes and edges, graph pooling can also simplify large-scale graphs, facilitating the application of GNNs in real-world problems (Defferrard et al., 2016; Ying et al., 2018b; Mesquita et al., 2020; Zhang et al., 2020b; Tsitsulin et al., 2023b). Therefore, understanding and enhancing graph pooling approaches is the key to increasing GNN performance, driving the progress of deep geometric learning.

In literature, existing graph pooling approaches can be roughly divided into two categories (Bianchi & Lachi, 2024; Liu et al., 2022a), i.e., node dropping pooling (Knyazev et al., 2019; Lee et al., 2019; Ranjan et al., 2020; Ma et al., 2020b; Zhang et al., 2020a; Zhou et al., 2022; Pang et al., 2021; Bacciu et al., 2023; Zhang et al., 2020a; 2019; Song et al., 2024) and node clustering pooling approaches (Ying et al., 2018a; Bianchi et al., 2020; Duval & Malliaros, 2022; Wu et al., 2022a; Hansen & Bianchi, 2023; Tsitsulin et al., 2023a; Bianchi, 2022), based on the strategies used to simplify the graph. node dropping pooling utilizes a learnable scoring function to remove nodes with relatively low significance scores, resulting in lower computational costs, while node clustering pooling approaches typically treat graph pooling as a node clustering problem, where clusters are considered

as new nodes for the coarsened graph (Liu et al., 2022b; Bianchi & Lachi, 2024). Even though graph pooling research is becoming increasingly popular, there is still no standardized benchmark that allows for an impartial and consistent comparison of various graph pooling methods. Furthermore, due to the diversity and complexity of graph datasets, numerous experimental settings have been used in previous studies, such as varied proportions of training data and train/validation/test splits (Bianchi et al., 2020; Hansen & Bianchi, 2023; Dwivedi et al., 2023; Xu et al., 2024b). As a result, a comprehensive and publicly available benchmark of graph pooling approaches is highly expected that can facilitate the evaluation and comparison of different approaches, ensuring the reproducibility of results and further advancing the area of graph machine learning.

Towards this end, we present a comprehensive graph pooling benchmark, which includes 17 graph pooling methods and 28 datasets across different graph machine learning problems. In particular, we extensively investigate graph pooling approaches across three key perspectives, i.e., *effectiveness*, *robustness*, and *generalizability*. To begin, we provide a fair and thorough *effectiveness* comparison of existing graph pooling approaches across graph classification, graph regression and node classification. Then, we evaluate the *robustness* of graph pooling approaches under both noise attacks on graph structures and node attributes. In addition, we study the *generalizability* of different approaches under out-of-distribution shifts from both size and density levels. Finally, we include efficiency comparison, parameter analysis and backbone analysis for completeness.

Based on extensive experimental results, we have made the following observations: (1) Node clustering pooling methods outperform node dropping pooling methods in terms of robustness, generalizability, and performance on graph regression tasks. (2) Node clustering pooling methods incur higher computational costs, and both approaches exhibit comparable performance on graph classification tasks. (3) AsymCheegerCutPool and ParsPool demonstrate strong performance in graph classification tasks. (4) As the scale of graph data decreases, the performance gap between different graph pooling methods in node classification tasks increases, with KMISPool and ParsPool exhibiting outstanding performance. (5) Most graph pooling approaches experience significant performance degradation due to distribution shifts and are also challenged by class imbalance issues, but the extent of this impact varies across different datasets. (6) Node clustering pooling is relatively superior to node dropping pooling in terms of robustness and generalizability, while KMISPool demonstrates relatively better robustness and generalizability in node dropping pooling methods.

The main contributions of this paper are as follows:

- *Comprehensive Benchmark.* We present a comprehensive graph pooling benchmark, which incorporates 17 state-of-the-art graph pooling approaches and 28 diverse datasets across graph classification, graph regression, and node classification.
- *Extensive Analysis.* To investigate the pros and cons of graph pooling approaches, we thoroughly evaluate current approaches from three perspectives, i.e., *effectiveness*, *robustness*, and *generalizability*, which can serve as guidance for researchers in different applications.
- *Open-source Material.* We have made our benchmark of all these graph pooling approaches available and reproducible, and we believe our benchmark can benefit researchers in both graph machine learning and interdisciplinary fields.

2 PRELIMINARIES

Notations. Consider a graph G characterized by a vertex set V and an edge set E . The features associated with each vertex are represented by the matrix $\mathbf{X} \in \mathbb{R}^{|V| \times d}$, where $|V|$ denotes the number of vertices, and d signifies the dimensionality of the attribute vectors. The adjacency relationships within the graph are encapsulated by the adjacency matrix $\mathbf{A} \in \{0, 1\}^{|V| \times |V|}$, where an entry $\mathbf{A}[i, j] = 1$ indicates the presence of an edge between vertex v_i and vertex v_j ; otherwise, $\mathbf{A}[i, j] = 0$.

Graph Pooling (Liu et al., 2022b; Grattarola et al., 2022b; Bianchi & Lachi, 2024). The aim of graph pooling is to reduce the spatial size of feature maps while preserving essential semantics, which thereby decreases computational complexity and memory usage. In this work, we focus on hierarchical pooling approaches (Ying et al., 2018b). Let POOL denote a graph pooling function

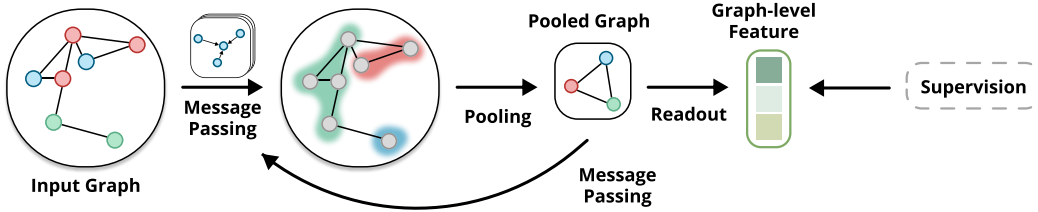


Figure 1: Overview of our hierarchical backbone for graph classification and graph regression.

which maps G to a graph $G' = (V', E')$ with the reduced size:

$$G' = \text{POOL}(G), \tag{1}$$

where $|V'| < |V|$. the process has two main principal components, i.e., *reduction*, and *connection* (Grattarola et al., 2022b). In particular, the reduction component aims to generate pooled nodes and their attributes in G' during the connection. The connection component computes the edges E' among the V' nodes.

Graph Classification and Regression (Knyazev et al., 2019; Chen et al., 2019; Grattarola et al., 2022b). The two primary graph-level tasks are graph regression and graph classification. Here, a graph dataset \mathcal{G} is provided as a set of graph-label pairs (G_i, y_i) , where y_i denotes the label for graph G_i . The objective is to train a powerful discriminative model f that predicts the correct label y_i given an input graph G_i . In graph classification, y_i are categorical labels $1, \dots, K$ with K as the number of classes, while in graph regression, y_i are continuous values. A well-trained graph classification model should output labels that closely match the true labels, and similarly, a graph regression model should predict values that are nearly identical to the ground truth values. In these tasks, graph pooling always accompanies graph convolutional operators. In formulation, the basic updating rule is written as follows:

$$\mathbf{H}^{(l+1)} = \sigma(\tilde{\mathbf{D}}^{-\frac{1}{2}} \tilde{\mathbf{A}} \tilde{\mathbf{D}}^{-\frac{1}{2}} \mathbf{H}^{(l)} \mathbf{W}^{(l)}), \tag{2}$$

where $\mathbf{H}^{(l)}$ denotes the node feature matrix at layer l , $\mathbf{W}^{(l)}$ denotes the weight matrix at the corresponding layer, $\tilde{\mathbf{A}} = \mathbf{A} + \mathbf{I}$ is the adjacency matrix \mathbf{A} plus the identity matrix \mathbf{I} , $\tilde{\mathbf{D}}$ is the degree matrix of $\tilde{\mathbf{A}}$, and σ is a nonlinear activation function (Kipf & Welling, 2016a). The pooling layers can be formulated as:

$$\mathbf{H}^{(pool)} = \text{POOL}(\mathbf{H}^{(L)}), \tag{3}$$

where $\mathbf{H}^{(pool)}$ is the node feature matrix after pooling. We iteratively conduct graph convolution and graph pooling operators and adopt a readout function to output the graph representation for downstream tasks. The overview of the basic hierarchical backbone can be found in Figure 1.

Node Classification (Kipf & Welling, 2016a; Veličković et al., 2018; Perozzi et al., 2014). The aim of node classification is to assign semantic labels to nodes in a graph according to their attributes and relationships with different nodes. Each dataset involves a graph G , consisting of nodes v_i and their corresponding labels y_i . $|V|$ is divided into a labeled set V^l and an unlabeled set V^u . We are required to train a graph neural network model that can predict the missing labels of nodes in V^u using the attributes of other nodes. U-Net framework (Ronneberger et al., 2015) is widely used to incorporate pooling operations for node classification. In the encoder part, U-Net progressively applies pooling and graph convolution to downsample the graphs and extract multi-scale features. The decoder part of U-Net utilizes upsampling and graph convolution to gradually upsample the low-resolution feature maps back to the original graph size. Residual connections are employed to directly transfer the feature maps from the encoder to the decoder, facilitating the preservation of fine-grained semantics during upsampling (Ronneberger et al., 2015; Ibtehaz & Rahman, 2020; Leng et al., 2018). For more information about the U-Net, please refer to Appendix B.

Table 1: Overview of experimental details of graph pooling research. These papers utilize different settings, which validates the necessity of building a comprehensive and fair benchmark.

Methods		Datasets	Tasks
<i>Node Dropping Pooling</i>			
TopKPool	NIPS'19	MNIST, COLLAB, PROTEINS, D&D	Graph Classification
SAGPool	ICML'19	D&D, PROTEINS, NCI1, NCI109, FRANKENSTEIN	Graph Classification
ASAPool	AAAI'20	D&D, PROTEINS, NCI1, NCI109, FRANKENSTEIN	Graph Classification
PANPool	NIPS'20	PROTEINS, PROTEINS_FULLL, NCI1, AIDS, MUTAGENCITY	Graph Classification
COPool	ECMLPKDD'22	BZR, AIDS, NCI1, NCI109, PROTEINS, QM7, IMDB-M	Graph Classification, Graph Regression
CGIPool	SIGIR'22	NCI1, NCI109, MUTAG, IMDB-B, IMDB-M, COLLAB, PROTEINS	Graph Classification
KMISPool	AAAI'23	D&D, REDDIT-B, REDDIT-5K, REDDIT-12K, Github	Graph Classification, Node Classification
GSAPool	WWW'20	D&D, NCI1, NCI109, MUTAG	Graph Classification
HGPSLPool	Arxiv'19	D&D, PROTEINS, NCI1, NCI109, ENZYMES, MUTAG	Graph Classification
<i>Node Clustering Pooling</i>			
AsymCheegerCutPool	ICML'23	Cora, Citeseer, Pubmed, DBLP	Node Classification
DiffPool	NIPS'18	D&D, PROTEINS, COLLAB, ENZYMES, REDDIT-MULTI	Graph Classification
MincutPool	ICML'20	D&D, PROTEINS, COLLAB, REDDIT-B, MUTAG, QM9	Graph Classification, Graph Regression
DMoNPool	JMLR'23	Cora, Citeseer Pubmed, Coauthor	Node Classification
HoscPool	CIKM'22	Cora, Citeseer Pubmed, Coauthor, DBLP, Email-EU	Node Classification
JustBalancePool	Arxiv'22	Cora, Citeseer, Pubmed, DBLP	Node Classification
SEPool	ICML'22	IMDB-B, IMDB-M, COLLAB, MUTAG, Cora, Citeseer, Pubmed	Graph Classification, Node Classification
ParsPool	ICLR'24	D&D, PROTEINS, NCI1, NCI109, Ogbg-molpcba, Cora, Citeseer, Pubmed	Graph Classification, Node Classification

3 GRAPH POOLING BENCHMARK

3.1 GRAPH POOLING APPROACHES

Our benchmark contains 17 state-of-the-art graph pooling approaches (detailed in Table 1): TopKPool (Knyazev et al., 2019), SAGPool (Lee et al., 2019), ASAPool (Ranjan et al., 2020), PANPool (Ma et al., 2020b), COPool (Zhou et al., 2022), CGIPool (Pang et al., 2021), KMISPool (Bacciu et al., 2023), GSAPool (Zhang et al., 2020a), HGPSLPool (Zhang et al., 2019), Asym-CheegerCutPool (Hansen & Bianchi, 2023), DiffPool (Ying et al., 2018a), MincutPool (Bianchi et al., 2020), DMoNPool (Tsitsulin et al., 2023a), HoscPool (Duval & Malliaros, 2022), JustBalancePool (Bianchi, 2022), SEPool (Wu et al., 2022a), and ParsPool (Song et al., 2024). More information related to the selected pooling methods can be found in the Appendix C.

3.2 DATASETS

To systematically evaluate graph pooling methods, we integrate 28 datasets from different domains. For graph classification, we select eleven publicly available datasets from TUDataset (Morris et al., 2020), including seven molecules datasets, i.e., MUTAG (Debnath et al., 1991), NCI1 (Wale et al., 2008), NCI109 (Wale et al., 2008), COX2 Sutherland et al. (2003), AIDS Riesen & Bunke (2008), FRANKENSTEIN Orsini et al. (2015), and Mutagenicity Debnath et al. (1991), four bioinformatics datasets, i.e. D&D (Shervashidze et al., 2011), PROTEINS (Borgwardt et al., 2005), PROTEINS_FULL (Borgwardt et al., 2005), and ENZYMES (Schomburg et al., 2004), three social network dataset, i.e., IMDB-BINARY (IMDB-B) (Cai & Wang, 2018), IMDB-MULTI (IMDB-M) (Cai & Wang, 2018), and COLLAB (Cai & Wang, 2018). We also include a large-scale graph classification dataset, Ogbg-molpcba, from the Open Graph Benchmark (OGB) (Hu et al., 2020b). For graph regression, we choose six datasets from MoleculeNet (Wu et al., 2018) including QM7, QM8, BACE, ESOL, FreeSolv, and Lipophilicity. For node classification, we utilize three citation networks, i.e., Cora, Citeseer, and Pubmed (Yang et al., 2016), three website networks, i.e., Cornell, Texas, and Wisconsin (Pei et al., 2020), and the GitHub dataset (Rozemberczki et al., 2021). We also obtain a large-scale dataset, Ogbn-arxiv, from OGB (Hu et al., 2020b). More information about the summary statistics and description of the datasets are detailed in the Appendix D.

3.3 EVALUATION PROTOCOLS

Our benchmark evaluation encompasses three key aspects, i.e., effectiveness, robustness, and generalizability. We perform a hyperparameter search for all pooling methods; detailed information can be found in Appendix E. *Firstly*, we conduct a performance comparison of graph pooling approaches across three tasks including graph classification, graph regression, and node classification. For graph and node classification tasks, we employ average precision for Ogbg-molpcba, and accuracy for remaining datasets as the evaluation metric. For graph regression, we use root mean square error (RMSE) for ESOL, FreeSolv, and Lipophilicity (Wu et al., 2018). Following previous research (Xu et al., 2024b), we use the area under the receiver operating characteristic (AUROC) curve to evaluate BACE, and mean absolute error (MAE) for QM7 and QM8. *Secondly*, our bench-

Table 2: Results of **graph classification** for different graph pooling methods. The mean and variance of average precision (Ogbg-molpcba) and accuracy (remaining datasets) are reported. The best and 2nd best are noted in bold font and underlined, respectively. OOM denotes out of GPU memory, and OOT denotes cannot be computed within 24 hours.

Methods	Ogbg-molpcba	PROTEINS	NCII	NCI109	MUTAG	D&D	IMDB-B	IMDB-M	COLLAB	Avg.	Rank
<i>Node Drop Pooling</i>											
TopKPool	15.79±0.42	70.83±1.25	70.34±1.80	69.65±1.61	82.76±4.88	69.07±5.52	74.44±3.71	48.44±3.46	75.38±1.13	70.11	12.44
SAGPool	21.08±2.19	74.64±1.53	73.10±1.21	71.29±0.82	81.61±5.86	73.27±1.12	75.33±3.31	48.74±3.09	77.91±2.22	71.99	8.06
ASAPool	OOT	73.69±1.48	73.48±1.03	70.45±0.84	72.41±10.15	OOT	71.56±3.46	46.96±3.72	OOT	68.09	13.56
PANPool	21.81±0.99	70.60±1.67	73.29±1.07	70.84±1.23	78.16±8.60	73.27±4.05	73.33±3.57	47.70±3.58	78.40±2.80	70.70	11.00
COPool	25.50±2.46	75.24±2.46	74.10±1.06	71.35±1.05	83.91±3.25	73.57±0.42	74.44±4.40	48.89±3.82	81.33±1.15	72.85	5.28
CGIPool	23.78±6.71	73.57±1.49	75.72±1.65	73.81±0.42	86.21±4.88	72.07±1.47	74.22±3.62	46.22±2.02	80.40±1.71	72.78	8.22
KMISPool	26.85±0.28	70.63±1.01	73.15±2.19	73.17±1.10	80.46±4.30	70.57±1.70	72.89±3.62	46.96±2.47	80.71±0.49	71.07	9.83
GSAPool	26.95±1.36	72.14±1.09	71.12±1.33	70.65±1.45	87.36±1.63	72.97±1.27	74.67±3.93	46.37±4.13	76.84±2.11	71.52	9.28
HGPSLPool	22.78±0.51	72.02±1.73	72.22±0.42	70.35±1.31	71.26±12.70	73.27±2.78	72.89±4.37	46.81±2.19	79.24±0.80	69.76	12.17
<i>Node Clustering Pooling</i>											
AsymCheegerCutPool	24.82±0.60	74.60±1.96	75.90±1.69	73.98±1.88	89.66±2.82	74.47±2.36	74.89±3.14	48.30±3.63	80.62±1.06	74.05	4.72
DiffPool	25.21±0.42	74.80±1.71	74.72±1.82	75.16±0.35	80.46±5.86	73.57±1.85	74.44±0.63	47.70±4.01	78.89±0.55	72.47	6.50
MincutPool	24.97±0.41	72.42±1.71	75.53±1.15	74.30±1.33	85.06±1.63	71.77±2.12	73.78±3.94	45.93±2.55	76.53±1.60	71.91	9.56
DMoNPool	24.75±0.67	68.45±4.79	72.45±0.15	71.18±1.66	75.86±5.63	75.38±0.42	73.33±3.81	47.26±1.68	77.07±0.44	70.12	11.17
HoscPool	24.63±0.37	72.42±0.74	76.88±0.61	76.13±1.97	85.06±1.63	71.77±2.12	74.67±1.96	45.93±2.77	78.18±1.69	72.63	8.06
JustBalancePool	25.19±0.42	68.85±2.97	76.34±0.46	76.34±1.51	81.61±1.63	71.77±2.12	74.89±4.09	45.93±5.08	77.87±1.26	71.70	8.67
SEPool	OOT	62.25±4.57	62.77±2.25	63.74±2.30	67.22±8.41	80.26±3.04	77.00±4.05	54.13±3.71	75.64±2.04	67.88	11.39
ParsPool	26.63±0.30	<u>75.02±0.64</u>	77.07±0.23	<u>76.20±0.44</u>	79.31±5.63	<u>76.10±0.80</u>	75.11±2.20	<u>49.48±0.91</u>	83.60±0.50	<u>73.99</u>	3.11

mark evaluates the robustness of graph pooling approaches in both graph-level and node-level tasks across two perspectives: structural robustness and feature robustness (Li & Wang, 2018). In particular, we add and drop edges of graphs to study structural robustness and mask node features to investigate feature robustness. *Thirdly*, we employ size-based and density-based distribution shifts to evaluate the generalizability of different pooling methods in graph-level tasks under real-world scenarios (Gui et al., 2022). We also use degree-based and closeness-based distribution shifts to assess the generalizability of different pooling methods in node-level tasks. In addition to these three views, we conduct a further analysis of these graph pooling approaches including the comparison of efficiency, visualization, and different backbone parameter choices.

4 EXPERIMENT

4.1 EXPERIMENTAL SETTINGS

All graph pooling methods in our benchmark are implemented by PyTorch (Paszke et al., 2019). Graph convolutional networks serve as the default encoders for all algorithms. The experimental setup includes a Linux server equipped with NVIDIA A100 GPUs, with an Intel Xeon Gold 6354 CPU. The software stack comprises PyTorch 1.11.0, PyTorch-geometric 2.1.0 (Fey & Lenssen, 2019), and Python 3.9.16. More details about experimental settings can be found in Appendix E.

4.2 EFFECTIVENESS ANALYSIS

Performance on Graph Classification. To begin, we investigate the performance of different graph pooling approaches on graph classification. The results of compared approaches on seven popular datasets are recorded in Table 2. *Firstly*, in general, ParsPool, AsymCheegerCutPool, and COPool are the three best-performing pooling models, and the performance of all 17 pooling methods varies significantly across different datasets. No single pooling method consistently outperforms the others across all datasets. *Secondly*, it is noteworthy that SEPool achieves significant advantages on D&D, IMDB-B, and IMDB-M. This is because SEPool’s coding tree structure, and these datasets are characterized by high clustering coefficients Watts & Strogatz (1998), which benefits the coding tree method because the hierarchical nature of the tree can better capture and represent these localized, highly connected substructures (Wu et al., 2022a). However, SEPool also implies greater computational resource overhead, which presents challenges when processing large-scale graph data such as Ogbg-molpcba. *Thirdly*, the methods with the highest average accuracy are ParsPool and AsymCheegerCutPool. ParsPool can capture a personalized pooling structure for each individual graph, while AsymCheegerCutPool calculates cluster assignments based on a tighter relaxation in terms of Graph Total Variation (GTV) (Song et al., 2024; Hansen & Bianchi, 2023). These methods are flexible, and the datasets differ significantly in diameter, degree, and clustering coefficients.

Table 3: Results of **graph regression** for different pooling methods. The mean and variance of MAE (QM7, QM8), AUROC (BACE), RMSE (ESOL, FreeSolv, Lipophilicity) are reported. - denotes cannot converge.

Methods	QM7	QM8	BACE	ESOL	FreeSolv	Lipophilicity	Rank
<i>Node Drop Pooling</i>							
TopKPool	63.39±9.66	0.021±0.001	0.85±0.02	0.96±0.06	1.92±0.37	0.80±0.02	8.1
SAGPool	97.69±11.19	0.023±0.001	0.84±0.01	1.16±0.07	2.31±0.66	0.93±0.06	13.1
ASAPool	56.79±6.17	0.029±0.008	0.85±0.02	0.92±0.03	1.92±0.37	0.78±0.05	8.2
PANPool	<u>53.04±1.20</u>	0.015±0.000	0.83±0.02	1.01±0.03	1.80±0.10	0.84±0.01	9.7
COPool	84.22±3.28	0.020±0.001	0.85±0.01	0.98±0.07	1.85±0.24	0.85±0.02	8.5
CGIPool	97.41±16.25	0.020±0.001	0.84±0.03	1.59±0.62	2.49±0.97	0.83±0.07	11.7
KMISPool	80.51±21.34	0.017±0.001	0.85±0.02	0.95±0.04	1.29±0.18	0.81±0.03	5.9
GSAPool	106.72±22.90	0.021±0.001	0.85±0.02	0.96±0.08	1.95±0.26	0.82±0.03	8.8
HGPSLPool	47.88±0.83	0.015±0.000	0.84±0.01	1.02±0.06	1.62±0.09	0.76±0.01	7.8
<i>Node Clustering Pooling</i>							
AsymCheegerCutPool	64.91±8.30	0.031 ± 0.005	0.84 ± 0.01	0.99 ± 0.12	2.00 ± 0.18	0.95 ± 0.11	12.9
DiffPool	54.98±3.44	0.037 ± 0.010	0.84 ± 0.02	0.81 ± 0.05	1.20 ± 0.09	0.73 ± 0.03	8.0
MincutPool	-	0.020 ± 0.001	0.85 ± 0.02	0.76 ± 0.02	1.19 ± 0.18	0.73 ± 0.02	4.3
DMoNPool	-	0.021 ± 0.001	0.85 ± 0.02	0.68 ± 0.02	<u>1.16 ± 0.15</u>	0.69 ± 0.02	3.5
HoscPool	59.44±21.48	0.019 ± 0.002	0.84 ± 0.01	0.76 ± 0.02	1.14 ± 0.13	0.72 ± 0.02	4.6
JustBalancePool	-	0.022 ± 0.004	0.85 ± 0.02	<u>0.74 ± 0.03</u>	1.26 ± 0.16	<u>0.70 ± 0.01</u>	4.9

Table 4: Results of **node classification** for different pooling methods. No Pooling denotes without pooling layers.

Methods	Ogbn-arxiv	Cora	Citeseer	Pubmed	Cornell	Texas	Wisconsin	Github	Avg. Rank
TopKPool	53.36±0.03	88.91±0.93	77.56±0.85	86.13±0.34	49.09±2.57	54.18±4.80	51.58±3.05	86.95±0.20	67.91 8.00
SAGPool	53.39±0.02	89.18±0.65	77.56±0.81	86.07±0.70	81.09±3.74	55.64±2.95	51.32±3.53	86.99±0.22	73.48 5.33
ASAPool	OOM	89.10±0.86	77.76±1.01	85.74±0.18	79.64±2.91	54.55±4.74	50.79±3.49	OOM	72.93 6.83
PANPool	OOM	89.05±0.96	77.20±0.98	85.88±0.11	78.91±2.47	56.36±5.14	50.53±3.18	OOM	72.99 8.00
COPool	OOM	89.00±0.70	77.26±0.89	85.27±0.27	77.82±3.13	56.36±5.98	52.37±2.68	86.68±0.20	73.01 7.50
CGIPool	53.60±0.39	89.15±0.84	77.40±0.81	85.92±0.66	81.82±4.30	54.55±4.15	51.05±3.85	86.88±0.22	73.32 6.33
KMISPool	53.38±0.08	89.74±0.02	77.75±0.01	87.80±0.01	79.56±1.31	81.42±1.64	82.31±0.50	87.09±0.04	83.10 2.50
GSAPool	53.76±0.11	89.05±0.77	77.16±0.92	86.21±0.73	80.36±3.71	54.18±3.88	51.84±4.29	87.12±0.09	73.13 6.67
HGPSLPool	OOM	89.08±0.83	77.84±0.67	OOM	58.55±3.71	55.27±3.37	51.58±1.75	OOM	69.71 6.33
SEPool	OOT	83.17±0.00	70.47±0.00	79.33±0.80	51.35±0.00	66.66±6.50	57.51±0.85	OOT	68.08 8.67
ParsPool	OOM	84.51±0.35	74.27±0.38	89.20±0.00	72.07±6.49	81.98±6.49	82.35±17.94	OOM	80.73 5.50
No Pooling	<u>53.61±0.07</u>	<u>89.48±0.27</u>	77.69±0.24	86.10±0.06	48.83±1.24	56.50±1.11	54.43±1.54	86.46±0.02	68.84 <u>5.17</u>

Performance on Graph Regression. We further explore the performance of different pooling methods through graph-level regression tasks. As shown in Table 3, we can observe that: *Firstly*, overall, node clustering pooling methods outperform node dropping pooling methods, with DMoNPool and MincutPool showing the best performance. The possible reason is that in graph regression tasks, the model’s objective is to predict a continuous numerical output. Such tasks typically require capturing global structural features and continuity within the graph. Compared to node clustering pooling, node dropping pooling tends to lose more global information (Tsitsulin et al., 2023a; Bianchi et al., 2020). DMoNPool and MincutPool are more inclined to maintain the global characteristics of the graph rather than emphasizing the representation of locally important structures, which may result in their performance being inferior to that of ParsPool, AsymCheegerCutPool, and COPool in graph classification tasks. *Secondly*, in the BACE dataset, the performance of most pooling methods tends to be consistent, whereas in other datasets, there is a greater variance in performance. The possible reason is that although the graphs in the BACE dataset are relatively large, the average diameter is relatively small, so different pooling methods face fewer challenges in summarizing the global structural information of the graphs, which may lead to more consistent performance.

Performance on Node Classification. Table 4 presents the performance of various pooling methods in node classification tasks. We observe the following: *Firstly*, KMISPool and ParsPool demonstrate the best overall performance, significantly outperforming other methods on small-scale datasets such as Cornell, Texas, and Wisconsin. *Secondly*, node classification models without pooling layers achieve comparable results to most pooling methods across the majority of datasets. A potential reason for this is that pooling operations tend to lose substantial node information, which consequently weakens performance in node classification tasks. *Thirdly*, the scalability of ASAPool, PANPool, HGPSLPool, SEPool, and ParsPool still requires improvement, as they face memory/runtime bottlenecks, making it cannot complete training on larger datasets such as Ogbn-arxiv or GitHub.

Table 5: Results of **graph classification under random noise attack** for different pooling methods.

Dataset	Ptb Method	TopKPool	SAGPool	ASAPool	PANPool	KMISPool	DiffPool	MincutPool	JustBalancePool
PROTEINS	ADD	73.58±5.77	72.76±3.87	74.59±3.74	39.63±42.27	71.14±0.57	73.78±2.59	72.36±2.92	75.00±1.49
	DROP	71.95±2.28	73.58±2.55	72.76±1.88	38.62±42.97	71.34±1.32	71.34±1.80	71.75±2.07	73.37±1.25
	MASK	72.56±3.11	73.78±3.45	71.14±2.55	72.88±4.71	72.97±2.24	72.97±0.29	72.36±3.24	70.12±2.28
NCI1	ADD	65.91±0.65	67.53±2.25	71.42±1.53	66.29±0.40	72.66±1.40	72.66±0.20	70.77±1.80	73.96±0.08
	DROP	63.16±1.52	61.64±1.46	64.07±0.73	65.53±1.31	73.58±3.00	66.18±2.22	65.05±0.73	64.18±1.61
	MASK	63.86±1.39	63.16±2.10	66.94±0.87	66.18±0.61	65.15±2.30	68.23±2.73	67.10±2.07	67.91±1.98
NCI109	ADD	66.18±0.73	68.55±1.13	69.62±2.11	64.84±2.74	75.32±0.99	73.33±0.97	71.34±2.89	71.29±2.79
	DROP	63.59±1.40	64.61±1.49	64.24±1.86	65.64±1.26	73.85±2.95	66.18±2.22	65.05±0.73	64.18±1.61
	MASK	65.22±1.97	66.61±0.92	65.65±1.08	66.29±0.91	66.34±1.85	66.99±2.71	68.23±0.47	66.61±3.43
MUTAG	ADD	86.21±5.63	79.31±2.82	75.86±10.15	68.97±4.88	80.46±4.30	72.41±9.75	78.16±4.30	68.97±4.88
	DROP	87.36±4.30	63.22±13.9	72.41±14.90	68.97±2.82	80.46±4.30	78.16±1.63	74.71±9.89	75.86±11.26
	MASK	78.16±16.26	64.37±9.05	60.92±7.09	71.26±3.25	83.91±8.13	78.16±4.30	77.01±3.25	70.11±4.30

Table 6: Results of **node classification under random noise attack** for different pooling methods.

Dataset	Ptb Method	TopKPool	SAGPool	ASAPool	PANPool	COPool	CGIPool	KMISPool	GSAPool	HGPSLPool
Cora	ADD	73.90±0.24	74.41±0.12	OOM	75.75±0.14	69.52±0.58	70.01±0.24	75.64±0.03	74.29±0.15	75.58±0.14
	DROP	85.01±0.09	85.45±0.36	85.40±0.19	85.11±0.20	85.06±0.13	85.04±0.23	85.83±0.21	85.30±0.33	85.60±0.19
	MASK	87.70±0.16	87.75±0.18	87.94±0.12	87.48±0.24	86.88±0.26	87.42±0.03	87.81±0.17	87.83±0.37	87.59±0.24
Citeseer	ADD	62.64±0.19	62.47±0.41	63.43±0.14	63.38±0.37	62.62±0.21	61.94±0.29	63.52±0.20	62.69±0.23	63.42±0.21
	DROP	75.31±0.26	75.50±0.19	75.81±0.04	75.52±0.10	75.18±0.46	75.34±0.12	76.54±0.32	75.32±0.29	76.00±0.21
	MASK	73.29±0.27	73.41±0.25	73.57±0.17	73.42±0.20	73.54±0.44	73.28±0.49	73.63±0.10	73.45±0.20	73.30±0.24
Pubmed	ADD	71.06±0.25	70.75±0.41	OOM	70.62±0.12	68.21±0.11	67.92±0.45	71.59±0.01	70.83±0.17	OOM
	DROP	85.46±0.09	86.03±0.12	OOM	85.55±0.04	85.68±0.04	85.59±0.13	85.30±0.06	85.59±0.06	OOM
	MASK	84.24±0.04	84.34±0.06	OOM	83.75±0.06	83.31±0.07	83.78±0.17	83.83±0.02	84.36±0.11	OOM

4.3 ROBUSTNESS ANALYSIS

The compared performance for three types of random noise on eight graph pooling methods on the PROTEINS, NCI1, NCI109, and MUTAG datasets are shown in Table 5. With a probability of 50%, edges of the graph are randomly removed or added, and node features are randomly masked. We can observe that: *Firstly*, overall, node clustering pooling demonstrates better robustness against three types of attacks compared to node dropping pooling. *Secondly*, among node dropping pooling methods, KMISPool generally performs the best. However, for small datasets such as MUTAG, TopKPool achieves the highest performance under noise attacks, because its node selection mechanism is less sensitive to local noise variations (Knyazev et al., 2019). *Thirdly*, noise attacking increases the performance fluctuations of pooling methods, making their prediction results more unstable. *Fourthly*, in larger datasets such as PROTEINS, NCI1, and NCI109, dropping edges has a greater impact on performance, whereas for MUTAG, masking node features has a more significant effect.

Table 6 presents the results of the robustness analysis for node-level tasks. From Table 6, we observe the following: *Firstly*, random attacks on the graph lead to a decrease in performance on node classification tasks, with different types of attacks causing varying degrees of performance degradation. Randomly adding edges has the most negative impact on performance, while randomly deleting edges has the least impact. *Secondly*, for larger graphs such as Cora, Citeseer, and Pubmed, KMISPool performs the best, whereas for smaller graphs such as Cornell, Texas, and Wisconsin, ASAPool performs better. Appendix F.1 provides results for the robustness analysis of node-level tasks.

As depicted in As shown in Figure 2, the model’s performance generally declines as the noise intensity increases. It is observed that, at the same level of noise, the impact on accuracy is more pronounced on smaller datasets Cora and CiteSeer, while it is relatively minor on larger dataset Pubmed. Among the three types of noise, although the accuracy of nearly all methods decreases amidst fluctuations, KMISPool and PANPool exhibit the strongest robustness, while COPool performs relatively poorly, despite the fact that most pooling methods show very similar performance.

4.4 GENERALIZABILITY ANALYSIS

Table 7 and Table 8 presents the performance of different graph pooling methods under out-of-distribution shifts. For the graph-level datasets D&D and NCI1, we implement two types of distribution shifts. The first type is based on the number of nodes, where the smallest 50% of graphs by node count are used as the training set, and the largest 20% as the test set, with the remainder serving as the validation set (Bevilacqua et al., 2021; Chen et al., 2022). Following the same criteria, the second type of out-of-distribution shifts are generated based on graph density (Chen et al., 2022).

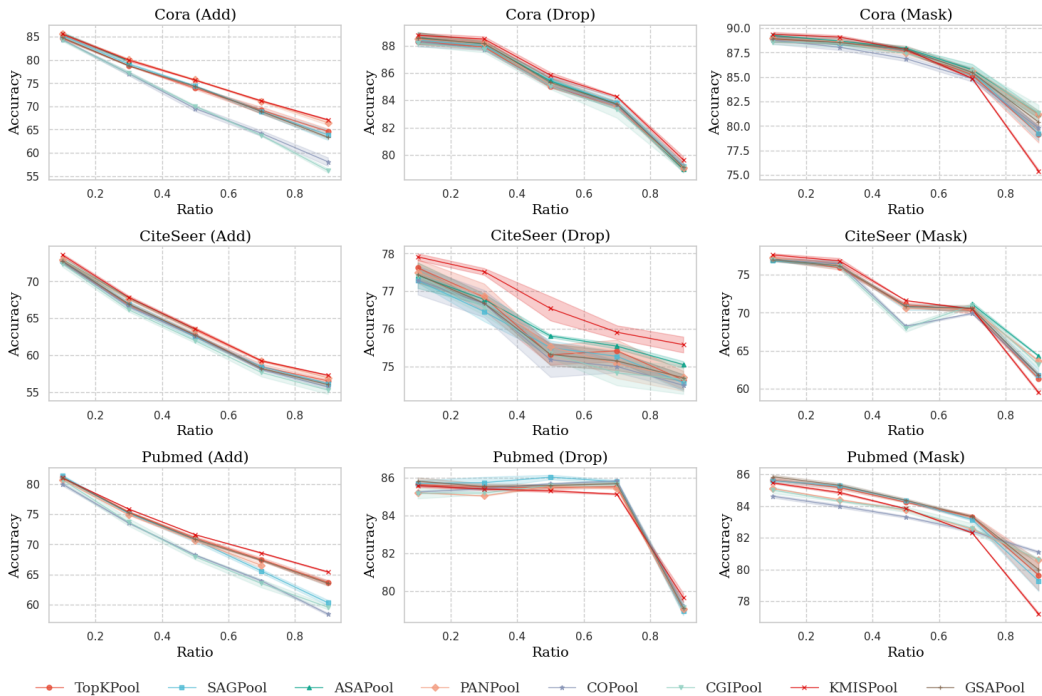


Figure 2: Performance of different approaches w.r.t. different rates of random noise.

Table 7: Results of **graph classification under distribution shifts**. Size and density denote two types of shifts across training and test datasets. Micro-F1 and Macro-F1 metrics are provided for each shift type.

Method	D&D				NCH			
	Size		Density		Size		Density	
	Micro-F1	Macro-F1	Micro-F1	Macro-F1	Micro-F1	Macro-F1	Micro-F1	Macro-F1
<i>Node Drop Pooling</i>								
TopKPool	68.08±1.60	63.69±1.13	31.98±15.37	29.43±15.16	25.89±0.46	24.98±0.43	53.48±2.11	51.02±3.14
SAGPool	81.36±2.49	74.47±1.48	55.37±0.89	50.14±0.97	25.08±2.39	23.90±2.95	47.00±3.60	45.86±3.49
ASAPool	OOT	OOT	OOT	OOT	26.29±3.66	25.29±4.42	53.17±1.85	51.34±1.18
PANPool	77.68±8.37	71.44±6.50	41.92±10.72	40.36±10.05	25.00±0.00	23.74±0.08	52.08±2.24	49.14±0.66
COPool	64.41±5.66	60.37±3.74	47.91±2.51	44.30±1.81	27.99±3.86	27.17±4.48	54.67±2.22	53.09±2.35
CGIPool	75.99±6.65	69.62±5.58	56.38±1.76	51.10±1.45	28.16±5.18	27.26±5.81	56.20±0.86	53.93±1.12
KMISPool	80.23±5.24	73.30±4.04	54.58±5.26	49.81±3.62	50.97±9.51	49.02±7.87	55.42±1.47	51.27±0.30
GSAPool	58.19±26.99	53.06±25.69	33.79±20.93	29.39±19.01	26.21±1.24	25.19±1.56	50.31±3.39	49.32±2.65
HGPSLPool	85.59±1.20	78.34±1.66	52.43±2.25	49.59±1.89	19.66±0.52	17.52±0.66	56.95±1.64	51.93±1.14
<i>Node Clustering Pooling</i>								
AsymCheegerCutPool	74.47±0.06	73.60±0.06	86.13±0.00	50.86±0.01	48.87±3.06	45.42±1.65	70.01±0.00	46.95±0.00
DiffPool	73.87±0.02	73.35±0.02	86.49±0.02	47.44±0.01	19.50±0.00	16.63±0.01	69.53±0.00	50.87±0.15
MincutPool	69.97±0.17	67.95±0.17	87.39±0.00	46.63±0.00	19.58±0.00	16.69±0.00	68.64±0.00	50.31±0.09
DMoNPool	72.67±0.11	72.25±0.13	82.52±0.00	54.21±0.00	79.29±0.04	64.30±0.00	68.92±0.00	48.76±0.02
HoscPool	70.27±0.01	69.20±0.00	87.39±0.00	46.63±0.00	24.60±0.27	23.39±0.36	70.48±0.01	56.55±0.35
JustBalancePool	68.77±0.00	67.82±0.02	87.39±0.00	46.63±0.00	19.98±0.00	17.28±0.01	68.64±0.00	50.31±0.09
ParsPool	68.36±1.60	62.50±1.76	63.06±4.84	48.35±0.86	52.59±4.46	49.95±3.32	56.27±1.97	52.96±0.88

For the node-level datasets Cora and Citeseer, the first type of out-of-distribution shift is the top 50% of nodes with the highest degrees as the training set, the bottom 25% with the lowest degrees as the test set, and the remaining nodes as the validation set. The second type is based on closeness centrality (the reciprocal of the sum of the shortest path lengths from a node to all other nodes). We use the 50% of nodes with the lowest closeness as the training set, the 25% with the highest closeness as the test set, and the remaining nodes as the validation set. For further details and more experiments for the generalizability analysis, please refer to the Appendix D.4 and Appendix F.2.

From Tables 7 and 8, we have the following observations. *Firstly*, node-level out-of-distribution shifts also reduce the performance of pooling models, but the extent of this reduction is smaller compared to out-of-distribution shifts in graph classification tasks. The potential reason is that, in node-level tasks, the propagation of information are usually confined to the local neighborhood of nodes, whereas graph-level tasks require handling information spread over a larger scope. *Secondly*,

Table 8: Results of **node classification under distribution shifts**. Degree and closeness denote two types of shifts across training and test datasets.

Method	Cora				Citeseer			
	Degree		Closeness		Degree		Closeness	
	Micro-F1	Macro-F1	Micro-F1	Macro-F1	Micro-F1	Macro-F1	Micro-F1	Macro-F1
TopKPool	83.65±0.50	82.29±0.47	83.21±0.18	81.98±0.31	67.27±0.35	63.60±0.26	72.28±0.67	65.64±1.00
SAGPool	84.19±0.12	82.73±0.27	81.68±1.54	80.34±1.55	65.46±0.61	62.22±0.49	72.28±1.10	66.35±1.87
ASAPool	83.16±0.00	82.24±0.13	84.10±0.37	82.97±0.32	67.47±0.23	63.94±0.31	72.84±0.49	65.27±1.74
PANPool	84.00±0.37	82.83±0.37	84.44±0.30	83.44±0.36	67.63±0.26	63.85±0.28	73.45±0.86	67.48±1.75
COPool	83.90±0.12	82.62±0.13	81.14±1.72	80.00±1.01	66.43±0.59	62.93±0.42	72.80±0.00	67.14±0.42
CGIPool	83.21±0.77	82.24±0.82	82.27±0.55	80.91±0.80	65.66±1.34	62.14±1.46	72.36±0.46	66.80±0.91
KMISPool	84.00±0.18	82.57±0.15	83.55±0.39	82.36±0.41	67.35±0.15	63.69±0.14	72.72±0.30	66.51±0.39
GSAPool	83.70±0.07	82.19±0.27	83.16±0.32	81.89±0.37	67.07±0.49	63.56±0.42	72.84±0.44	66.33±0.37
HGPSLPool	84.19±0.00	82.83±0.04	83.46±0.79	82.32±0.89	67.67±0.15	64.13±0.16	73.20±0.46	67.95±0.40

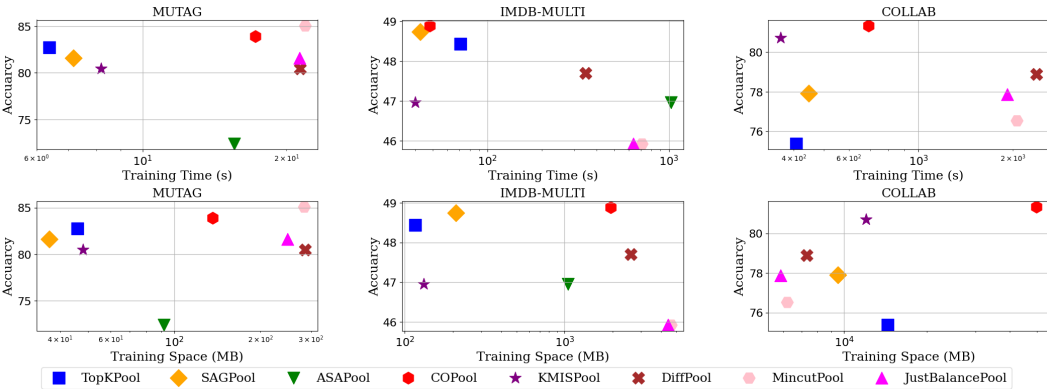


Figure 3: Comparison of performance, training time, and memory usage across different approaches.

Macro-F1 is generally lower than Micro-F1, which indicates that the model has weaker recognition capabilities for minority classes. *Thirdly*, node clustering pooling exhibits better generalizability than node dropping pooling in graph classification tasks. *Fourthly*, HGPSLPool and PANPool exhibit the best performance, potentially due to the fact that HGPSLPool combines graph convolution with spectral clustering, enabling it to better capture higher-order relationships and local topological structures, which is advantageous in node-level tasks. Meanwhile, PANPool utilizes an adaptive pooling strategy that adjusts the pooling method to suit different node feature distributions, enhancing the model’s robustness and generalization capability under out-of-distribution conditions.

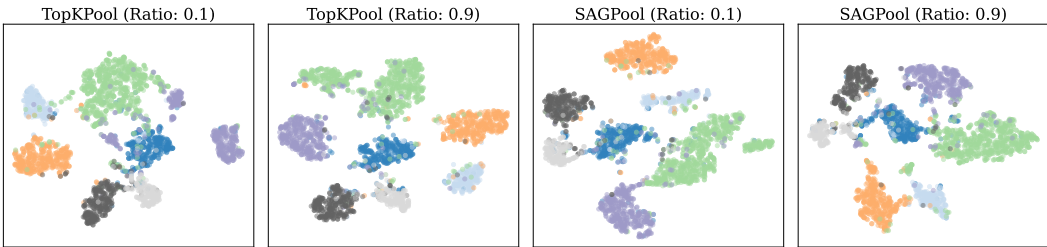


Figure 4: The t-SNE visualization w.r.t. different pooling ratios of TopKPool and SAGPool.

4.5 FURTHER ANALYSIS

Efficiency Comparison. In this part, we conduct an efficiency analysis of graph pooling methods on the MUTAG, IMDB-MULTI, and COLLAB datasets. We calculate the time of the algorithms by measuring the duration needed to complete 200 epochs of training with the 512 batch size. For space efficiency, we compute the GPU memory utilization during the training process. From Figure 3, it can be observed that ASAPool, DiffPool, MincutPool, and JustBalancePool exhibit significantly higher time and space costs. In contrast, node dropping pooling methods such as TopKPool, SAG-

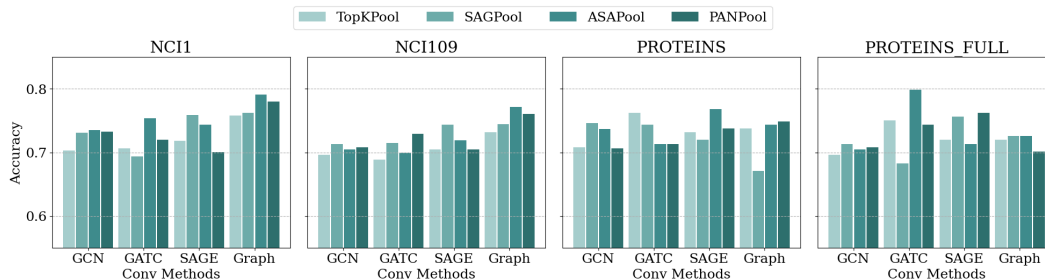


Figure 5: Performance w.r.t. graph convolution backbones for different pooling methods.

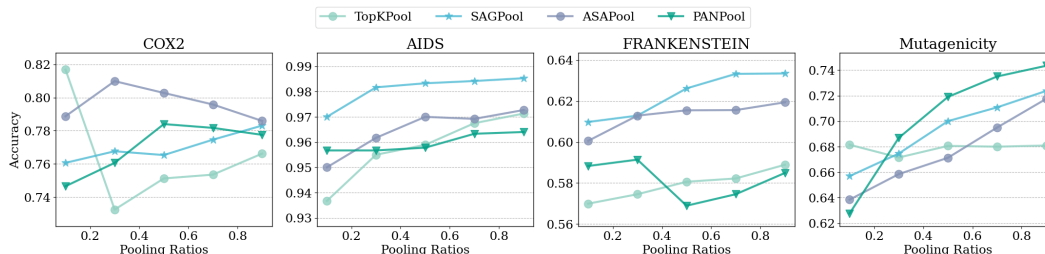


Figure 6: Performance w.r.t. different pooling ratios for four pooling methods.

Pool, and KMISPool demonstrate lower time and space costs. The underlying reason is that node clustering pooling methods require converting graph data into an adjacency matrix form and simplifying the graph through clustering rather than directly removing nodes.

Visualization. Figure 4 shows the t-SNE visualization for TopKPool and SAGPool under different pooling ratios. From the results, we observe that as the pooling ratio increases from 0.1 to 0.9, the different classes form more distinct clusters in the t-SNE plot when the pooling ratio is low. As the pooling ratio increases, the model retains more nodes, leading to a greater overlap between nodes of different classes and a reduction in inter-class separability. Moreover, when the pooling ratio is 0.9, SAGPool shows a higher degree of class separability compared to TopKPool.

Backbone Analysis. Figure 5 presents the performance of four pooling methods based on GCN-Conv (Kipf & Welling, 2016b), GATConv (Veličković et al., 2017), SAGEConv (Hamilton et al., 2017), and GraphConv (Morris et al., 2019) on four datasets, NCI1, NCI109, PROTEINS, and PROTEINS_FULL. On average, as the backbone models change, most pooling methods exhibit significant performance fluctuations, and no single backbone model consistently maintains a leading position. Except for the PROTEINS_FULL, the performance of GraphConv is relatively better.

Parameter Analysis. Figure 6 shows the performance of four pooling methods on the COX2, AIDS, FRANKENSTEIN, and Mutagenicity datasets. From the results, we observe that as the pooling rate increases from 0.1 to 0.9, the performance increases before reaching saturation in most cases. The performance variation among different pooling methods is significant as the pooling ratio changes, it is necessary to adjust the pooling ratio when employing pooling methods.

5 CONCLUSION

In this paper, we construct the first graph pooling benchmark that includes 17 state-of-the-art approaches and 28 different graph datasets across graph classification, graph regression, and node classification. We find that node clustering pooling methods outperform node dropping pooling methods in terms of robustness and generalizability, but at the cost of higher computational expenses. This benchmark systematically analyzes the effectiveness, robustness, and generalizability of graph pooling methods. We also make our benchmark publicly available to advance the fields of graph machine learning and applications. One limitation of our benchmark is the lack of more complicated settings under label scarcity. In future works, we would extend our graph pooling benchmark to more realistic settings such as semi-supervised learning and few-shot learning.

REFERENCES

- 540
541
542 Emily Alsentzer, Samuel Finlayson, Michelle Li, and Marinka Zitnik. Subgraph neural networks.
543 *Advances in Neural Information Processing Systems*, 33:8017–8029, 2020.
- 544 Davide Bacciu, Alessio Conte, and Francesco Landolfi. Generalizing downsampling from regular
545 data to graphs. In *Proceedings of the AAAI Conference on Artificial Intelligence*, volume 37, pp.
546 6718–6727, 2023.
- 547 Jinheon Baek, Minki Kang, and Sung Ju Hwang. Accurate learning of graph representations with
548 graph multiset pooling. *arXiv preprint arXiv:2102.11533*, 2021.
- 549
550 Beatrice Bevilacqua, Yangze Zhou, and Bruno Ribeiro. Size-invariant graph representations for
551 graph classification extrapolations. In *International Conference on Machine Learning*, pp. 837–
552 851. PMLR, 2021.
- 553 Smriti Bhagat, Graham Cormode, and S Muthukrishnan. Node classification in social networks.
554 *Social network data analytics*, pp. 115–148, 2011.
- 555
556 Tian Bian, Xi Xiao, Tingyang Xu, Peilin Zhao, Wenbing Huang, Yu Rong, and Junzhou Huang. Ru-
557 mor detection on social media with bi-directional graph convolutional networks. In *Proceedings*
558 *of the AAAI conference on artificial intelligence*, volume 34, pp. 549–556, 2020.
- 559 Filippo Maria Bianchi. Simplifying clustering with graph neural networks. *arXiv preprint*
560 *arXiv:2207.08779*, 2022.
- 561
562 Filippo Maria Bianchi and Veronica Lachi. The expressive power of pooling in graph neural net-
563 works. *Advances in Neural Information Processing Systems*, 36, 2024.
- 564 Filippo Maria Bianchi, Daniele Grattarola, and Cesare Alippi. Spectral clustering with graph neural
565 networks for graph pooling. In *International conference on machine learning*, pp. 874–883.
566 PMLR, 2020.
- 567
568 Karsten M Borgwardt, Cheng Soon Ong, Stefan Schönauer, SVN Vishwanathan, Alex J Smola, and
569 Hans-Peter Kriegel. Protein function prediction via graph kernels. *Bioinformatics*, 21(suppl_1):
570 i47–i56, 2005.
- 571
572 Chen Cai and Yusu Wang. A simple yet effective baseline for non-attributed graph classification.
573 *arXiv preprint arXiv:1811.03508*, 2018.
- 574 David Camacho, Angel Panizo-LLedot, Gema Bello-Orgaz, Antonio Gonzalez-Pardo, and Erik
575 Cambria. The four dimensions of social network analysis: An overview of research methods,
576 applications, and software tools. *Information Fusion*, 63:88–120, 2020.
- 577
578 Ting Chen, Song Bian, and Yizhou Sun. Are powerful graph neural nets necessary? a dissection on
579 graph classification. *arXiv preprint arXiv:1905.04579*, 2019.
- 580 Yongqiang Chen, Yonggang Zhang, Yatao Bian, Han Yang, MA Kaili, Binghui Xie, Tongliang Liu,
581 Bo Han, and James Cheng. Learning causally invariant representations for out-of-distribution
582 generalization on graphs. *Advances in Neural Information Processing Systems*, 35:22131–22148,
583 2022.
- 584 Edward Choi, Zhen Xu, Yujia Li, Michael Dusenberry, Gerardo Flores, Emily Xue, and Andrew Dai.
585 Learning the graphical structure of electronic health records with graph convolutional transformer.
586 In *Proceedings of the AAAI conference on artificial intelligence*, volume 34, pp. 606–613, 2020.
- 587
588 Myriam Ciordia, Laura Pérez-Benito, Francisca Delgado, Andrés A Trabanco, and Gary Tresadern.
589 Application of free energy perturbation for the design of bace1 inhibitors. *Journal of Chemical*
590 *information and modeling*, 56(9):1856–1871, 2016.
- 591
592 Asim Kumar Debnath, Rosa L Lopez de Compadre, Gargi Debnath, Alan J Shusterman, and Cor-
593 win Hansch. Structure-activity relationship of mutagenic aromatic and heteroaromatic nitro com-
pounds. correlation with molecular orbital energies and hydrophobicity. *Journal of medicinal*
chemistry, 34(2):786–797, 1991.

- 594 Michaël Defferrard, Xavier Bresson, and Pierre Vandergheynst. Convolutional neural networks on
595 graphs with fast localized spectral filtering. *Advances in neural information processing systems*,
596 29, 2016.
- 597 John S Delaney. Esol: estimating aqueous solubility directly from molecular structure. *Journal of*
598 *chemical information and computer sciences*, 44(3):1000–1005, 2004.
- 600 Alexandre Duval and Fragkiskos Malliaros. Higher-order clustering and pooling for graph neural
601 networks. In *Proceedings of the 31st ACM International Conference on Information & Knowledge*
602 *Management*, pp. 426–435, 2022.
- 603 Vijay Prakash Dwivedi, Chaitanya K Joshi, Anh Tuan Luu, Thomas Laurent, Yoshua Bengio, and
604 Xavier Bresson. Benchmarking graph neural networks. *Journal of Machine Learning Research*,
605 24(43):1–48, 2023.
- 607 Federico Errica, Marco Podda, Davide Bacciu, and Alessio Micheli. A fair comparison of graph
608 neural networks for graph classification. *arXiv preprint arXiv:1912.09893*, 2019.
- 609 Matthias Fey and Jan E. Lenssen. Fast graph representation learning with PyTorch Geometric. In
610 *ICLR Workshop on Representation Learning on Graphs and Manifolds*, 2019.
- 612 Hongyang Gao and Shuiwang Ji. Graph u-nets. In *international conference on machine learning*,
613 pp. 2083–2092. PMLR, 2019.
- 614 Daniele Grattarola, Daniele Zambon, Filippo Maria Bianchi, and Cesare Alippi. Understanding
615 pooling in graph neural networks. *IEEE transactions on neural networks and learning systems*,
616 2022a.
- 618 Daniele Grattarola, Daniele Zambon, Filippo Maria Bianchi, and Cesare Alippi. Understanding
619 pooling in graph neural networks. *IEEE transactions on neural networks and learning systems*,
620 2022b.
- 621 Shurui Gui, Xiner Li, Limei Wang, and Shuiwang Ji. Good: A graph out-of-distribution benchmark.
622 *Advances in Neural Information Processing Systems*, 35:2059–2073, 2022.
- 624 Will Hamilton, Zhitao Ying, and Jure Leskovec. Inductive representation learning on large graphs.
625 *Advances in neural information processing systems*, 30, 2017.
- 626 Jonas Berg Hansen and Filippo Maria Bianchi. Total variation graph neural networks. In *International*
627 *Conference on Machine Learning*, pp. 12445–12468. PMLR, 2023.
- 629 Weihua Hu, Matthias Fey, Marinka Zitnik, Yuxiao Dong, Hongyu Ren, Bowen Liu, Michele Catasta,
630 and Jure Leskovec. Open graph benchmark: Datasets for machine learning on graphs. *Advances*
631 *in neural information processing systems*, 33:22118–22133, 2020a.
- 633 Weihua Hu, Matthias Fey, Marinka Zitnik, Yuxiao Dong, Hongyu Ren, Bowen Liu, Michele Catasta,
634 and Jure Leskovec. Open graph benchmark: Datasets for machine learning on graphs. *Advances*
635 *in neural information processing systems*, 33:22118–22133, 2020b.
- 636 Nabil Ibtehaz and M Sohel Rahman. Multiresunet: Rethinking the u-net architecture for multimodal
637 biomedical image segmentation. *Neural networks*, 121:74–87, 2020.
- 638 Wei Ju, Siyu Yi, Yifan Wang, Qingqing Long, Junyu Luo, Zhiping Xiao, and Ming Zhang. A survey
639 of data-efficient graph learning, 2024.
- 641 Thomas N Kipf and Max Welling. Semi-supervised classification with graph convolutional net-
642 works. *arXiv preprint arXiv:1609.02907*, 2016a.
- 643 Thomas N Kipf and Max Welling. Semi-supervised classification with graph convolutional net-
644 works. *arXiv preprint arXiv:1609.02907*, 2016b.
- 645 Boris Knyazev, Graham W Taylor, and Mohamed Amer. Understanding attention and generalization
646 in graph neural networks. *Advances in neural information processing systems*, 32, 2019.

- 648 Junhyun Lee, Inyeop Lee, and Jaewoo Kang. Self-attention graph pooling. In *International confer-*
649 *ence on machine learning*, pp. 3734–3743. PMLR, 2019.
- 650
- 651 Jiaxu Leng, Ying Liu, Tianlin Zhang, Pei Quan, and Zhenyu Cui. Context-aware u-net for
652 biomedical image segmentation. In *2018 IEEE International Conference on Bioinformatics and*
653 *Biomedicine (BIBM)*, pp. 2535–2538. IEEE, 2018.
- 654 Tao Li and Jiexiang Wang. Distributed averaging with random network graphs and noises. *IEEE*
655 *Transactions on Information Theory*, 64(11):7063–7080, 2018.
- 656
- 657 Zhixun Li, Xin Sun, Yifan Luo, Yanqiao Zhu, Dingshuo Chen, Yingtao Luo, Xiangxin Zhou, Qiang
658 Liu, Shu Wu, Liang Wang, et al. Gslb: The graph structure learning benchmark. *Advances in*
659 *Neural Information Processing Systems*, 36, 2024.
- 660 Chuang Liu, Yibing Zhan, Jia Wu, Chang Li, Bo Du, Wenbin Hu, Tongliang Liu, and Dacheng Tao.
661 Graph pooling for graph neural networks: Progress, challenges, and opportunities. *arXiv preprint*
662 *arXiv:2204.07321*, 2022a.
- 663
- 664 Chuang Liu, Yibing Zhan, Jia Wu, Chang Li, Bo Du, Wenbin Hu, Tongliang Liu, and Dacheng Tao.
665 Graph pooling for graph neural networks: Progress, challenges, and opportunities. *arXiv preprint*
666 *arXiv:2204.07321*, 2022b.
- 667 Meng Liu, Hongyang Gao, and Shuiwang Ji. Towards deeper graph neural networks. In *Proceedings*
668 *of the 26th ACM SIGKDD international conference on knowledge discovery & data mining*, pp.
669 338–348, 2020.
- 670
- 671 Nina Lukashina, Alisa Alenicheva, Elizaveta Vlasova, Artem Kondiukov, Aigul Khakimova, Emil
672 Magerramov, Nikita Churikov, and Aleksei Shpilman. Lipophilicity prediction with multitask
673 learning and molecular substructures representation. *arXiv preprint arXiv:2011.12117*, 2020.
- 674 Chen Ma, Liheng Ma, Yingxue Zhang, Jianing Sun, Xue Liu, and Mark Coates. Memory augmented
675 graph neural networks for sequential recommendation. In *Proceedings of the AAAI conference on*
676 *artificial intelligence*, volume 34, pp. 5045–5052, 2020a.
- 677
- 678 Zheng Ma, Junyu Xuan, Yu Guang Wang, Ming Li, and Pietro Liò. Path integral based convolution
679 and pooling for graph neural networks. *Advances in Neural Information Processing Systems*, 33:
680 16421–16433, 2020b.
- 681 Diego Mesquita, Amauri Souza, and Samuel Kaski. Rethinking pooling in graph neural networks.
682 *Advances in Neural Information Processing Systems*, 33:2220–2231, 2020.
- 683
- 684 Caitlyn L Mills, Rohan Garg, Joslynn S Lee, Liang Tian, Alexandru Suciuc, Gene D Cooperman,
685 Penny J Beuning, and Mary Jo Ondrechen. Functional classification of protein structures by local
686 structure matching in graph representation. *Protein Science*, 27(6):1125–1135, 2018.
- 687 David L Mobley and J Peter Guthrie. Freesolv: a database of experimental and calculated hydration
688 free energies, with input files. *Journal of computer-aided molecular design*, 28:711–720, 2014.
- 689
- 690 Grégoire Montavon, Matthias Rupp, Vivekanand Gobre, Alvaro Vazquez-Mayagoitia, Katja Hansen,
691 Alexandre Tkatchenko, Klaus-Robert Müller, and O Anatole Von Lilienfeld. Machine learning
692 of molecular electronic properties in chemical compound space. *New Journal of Physics*, 15(9):
693 095003, 2013.
- 694 Christopher Morris, Martin Ritzert, Matthias Fey, William L Hamilton, Jan Eric Lenssen, Gaurav
695 Rattan, and Martin Grohe. Weisfeiler and leman go neural: Higher-order graph neural networks.
696 In *Proceedings of the AAAI conference on artificial intelligence*, volume 33, pp. 4602–4609, 2019.
- 697 Christopher Morris, Nils M Kriege, Franka Bause, Kristian Kersting, Petra Mutzel, and Marion
698 Neumann. Tudataset: A collection of benchmark datasets for learning with graphs. *arXiv preprint*
699 *arXiv:2007.08663*, 2020.
- 700
- 701 Ghaith Mqawass and Petr Popov. graphlambda: Fusion graph neural networks for binding affinity
prediction. *Journal of Chemical Information and Modeling*, 2024.

- 702 Francesco Orsini, Paolo Frasconi, and Luc De Raedt. Graph invariant kernels. In *Twenty-Fourth*
703 *International Joint Conference on Artificial Intelligence*, 2015.
- 704
- 705 Yunsheng Pang, Yunxiang Zhao, and Dongsheng Li. Graph pooling via coarsened graph infomax.
706 In *Proceedings of the 44th International ACM SIGIR Conference on Research and Development*
707 *in Information Retrieval*, pp. 2177–2181, 2021.
- 708 Adam Paszke, Sam Gross, Francisco Massa, Adam Lerer, James Bradbury, Gregory Chanan, Trevor
709 Killeen, Zeming Lin, Natalia Gimelshein, Luca Antiga, et al. Pytorch: An imperative style, high-
710 performance deep learning library. *Advances in neural information processing systems*, 32, 2019.
- 711
- 712 Hongbin Pei, Bingzhe Wei, Kevin Chen-Chuan Chang, Yu Lei, and Bo Yang. Geom-gcn: Geometric
713 graph convolutional networks. *arXiv preprint arXiv:2002.05287*, 2020.
- 714 Bryan Perozzi, Rami Al-Rfou, and Steven Skiena. Deepwalk: Online learning of social repre-
715 sentations. In *Proceedings of the 20th ACM SIGKDD international conference on Knowledge*
716 *discovery and data mining*, pp. 701–710, 2014.
- 717
- 718 Lianke Qin, Zhao Song, and Baocheng Sun. Is solving graph neural tangent kernel equivalent to
719 training graph neural network? *arXiv preprint arXiv:2309.07452*, 2023.
- 720 Ekagra Ranjan, Soumya Sanyal, and Partha Talukdar. Asap: Adaptive structure aware pooling for
721 learning hierarchical graph representations. In *Proceedings of the AAAI conference on artificial*
722 *intelligence*, volume 34, pp. 5470–5477, 2020.
- 723
- 724 Kaspar Riesen and Horst Bunke. Iam graph database repository for graph based pattern recognition
725 and machine learning. In *Structural, Syntactic, and Statistical Pattern Recognition: Joint IAPR*
726 *International Workshop, SSPR & SPR 2008, Orlando, USA, December 4-6, 2008. Proceedings*,
727 pp. 287–297. Springer, 2008.
- 728 Olaf Ronneberger, Philipp Fischer, and Thomas Brox. U-net: Convolutional networks for biomed-
729 ical image segmentation. In *Medical image computing and computer-assisted intervention—*
730 *MICCAI 2015: 18th international conference, Munich, Germany, October 5-9, 2015, proceed-*
731 *ings, part III 18*, pp. 234–241. Springer, 2015.
- 732
- 733 Benedek Rozemberczki, Carl Allen, and Rik Sarkar. Multi-scale attributed node embedding. *Journal*
734 *of Complex Networks*, 9(2):cnab014, 2021.
- 735 Ida Schomburg, Antje Chang, Christian Ebeling, Marion Gremse, Christian Heldt, Gregor Huhn,
736 and Dietmar Schomburg. Brenda, the enzyme database: updates and major new developments.
737 *Nucleic acids research*, 32(suppl_1):D431–D433, 2004.
- 738
- 739 Nino Shervashidze, Pascal Schweitzer, Erik Jan Van Leeuwen, Kurt Mehlhorn, and Karsten M Borg-
740 wardt. Weisfeiler-lehman graph kernels. *Journal of Machine Learning Research*, 12(9), 2011.
- 741 Nahian Siddique, Sidike Paheding, Colin P Elkin, and Vijay Devabhaktuni. U-net and its variants for
742 medical image segmentation: A review of theory and applications. *Ieee Access*, 9:82031–82057,
743 2021.
- 744
- 745 Yunchong Song, Siyuan Huang, Xinbing Wang, Chenghu Zhou, and Zhouhan Lin. Graph parsing
746 networks. *arXiv preprint arXiv:2402.14393*, 2024.
- 747 Mengzhu Sun, Xi Zhang, Jiaqi Zheng, and Guixiang Ma. Ddgc: Dual dynamic graph convolutional
748 networks for rumor detection on social media. In *Proceedings of the AAAI conference on artificial*
749 *intelligence*, volume 36, pp. 4611–4619, 2022.
- 750 Jeffrey J Sutherland, Lee A O’Brien, and Donald F Weaver. Spline-fitting with a genetic algorithm:
751 A method for developing classification structure- activity relationships. *Journal of chemical in-*
752 *formation and computer sciences*, 43(6):1906–1915, 2003.
- 753
- 754 Cheng Tan, Siyuan Li, Zhangyang Gao, Wenfei Guan, Zedong Wang, Zicheng Liu, Lirong Wu,
755 and Stan Z Li. Openstl: A comprehensive benchmark of spatio-temporal predictive learning.
Advances in Neural Information Processing Systems, 36:69819–69831, 2023.

- 756 Anton Tsitsulin, John Palowitch, Bryan Perozzi, and Emmanuel Müller. Graph clustering with graph
757 neural networks. *Journal of Machine Learning Research*, 24(127):1–21, 2023a.
- 758
759 Anton Tsitsulin, John Palowitch, Bryan Perozzi, and Emmanuel Müller. Graph clustering with graph
760 neural networks. *Journal of Machine Learning Research*, 24(127):1–21, 2023b.
- 761
762 Petar Veličković, Guillem Cucurull, Arantxa Casanova, Adriana Romero, Pietro Lio, and Yoshua
763 Bengio. Graph attention networks. *arXiv preprint arXiv:1710.10903*, 2017.
- 764
765 Petar Veličković, William Fedus, William L Hamilton, Pietro Liò, Yoshua Bengio, and R Devon
766 Hjelm. Deep graph infomax. *arXiv preprint arXiv:1809.10341*, 2018.
- 767
768 Nikil Wale, Ian A Watson, and George Karypis. Comparison of descriptor spaces for chemical
769 compound retrieval and classification. *Knowledge and Information Systems*, 14:347–375, 2008.
- 770
771 Duncan J Watts and Steven H Strogatz. Collective dynamics of ‘small-world’ networks. *nature*, 393
772 (6684):440–442, 1998.
- 773
774 Oliver Wieder, Stefan Kohlbacher, Méline Kuenemann, Arthur Garon, Pierre Ducrot, Thomas Sei-
775 del, and Thierry Langer. A compact review of molecular property prediction with graph neural
776 networks. *Drug Discovery Today: Technologies*, 37:1–12, 2020.
- 777
778 Junran Wu, Xueyuan Chen, Ke Xu, and Shangzhe Li. Structural entropy guided graph hierarchical
779 pooling. In *International conference on machine learning*, pp. 24017–24030. PMLR, 2022a.
- 780
781 Lingfei Wu, Peng Cui, Jian Pei, Liang Zhao, and Xiaojie Guo. Graph neural networks: foundation,
782 frontiers and applications. In *Proceedings of the 28th ACM SIGKDD Conference on Knowledge
783 Discovery and Data Mining*, pp. 4840–4841, 2022b.
- 784
785 Yongji Wu, Defu Lian, Yiheng Xu, Le Wu, and Enhong Chen. Graph convolutional networks
786 with markov random field reasoning for social spammer detection. In *Proceedings of the AAAI
787 conference on artificial intelligence*, volume 34, pp. 1054–1061, 2020a.
- 788
789 Zhenqin Wu, Bharath Ramsundar, Evan N Feinberg, Joseph Gomes, Caleb Geniesse, Aneesh S
790 Pappu, Karl Leswing, and Vijay Pande. Moleculenet: a benchmark for molecular machine learn-
791 ing. *Chemical science*, 9(2):513–530, 2018.
- 792
793 Zonghan Wu, Shirui Pan, Fengwen Chen, Guodong Long, Chengqi Zhang, and S Yu Philip. A
794 comprehensive survey on graph neural networks. *IEEE transactions on neural networks and
795 learning systems*, 32(1):4–24, 2020b.
- 796
797 Shunxin Xiao, Shiping Wang, Yuanfei Dai, and Wenzhong Guo. Graph neural networks in node
798 classification: survey and evaluation. *Machine Vision and Applications*, 33(1):4, 2022.
- 799
800 Fanding Xu, Zhiwei Yang, Lizhuo Wang, Deyu Meng, and Jiangang Long. Mespool: Molecular
801 edge shrinkage pooling for hierarchical molecular representation learning and property prediction.
802 *Briefings in Bioinformatics*, 25(1):bbad423, 2024a.
- 803
804 Fanding Xu, Zhiwei Yang, Lizhuo Wang, Deyu Meng, and Jiangang Long. Mespool: Molecular
805 edge shrinkage pooling for hierarchical molecular representation learning and property prediction.
806 *Briefings in Bioinformatics*, 25(1):bbad423, 2024b.
- 807
808 Liangwei Yang, Zhiwei Liu, Yingdong Dou, Jing Ma, and Philip S Yu. Consisrec: Enhancing
809 gnn for social recommendation via consistent neighbor aggregation. In *Proceedings of the 44th
international ACM SIGIR conference on Research and development in information retrieval*, pp.
2141–2145, 2021.
- 806
807 Zhilin Yang, William Cohen, and Ruslan Salakhudinov. Revisiting semi-supervised learning with
808 graph embeddings. In *International conference on machine learning*, pp. 40–48. PMLR, 2016.
- 809
809 Zi Ye, Yogan Jaya Kumar, Goh Ong Sing, Fengyan Song, and Junsong Wang. A comprehensive
survey of graph neural networks for knowledge graphs. *IEEE Access*, 10:75729–75741, 2022.

- 810 Zhitao Ying, Jiaxuan You, Christopher Morris, Xiang Ren, Will Hamilton, and Jure Leskovec. Hier-
811 archical graph representation learning with differentiable pooling. *Advances in neural information*
812 *processing systems*, 31, 2018a.
- 813
814 Zhitao Ying, Jiaxuan You, Christopher Morris, Xiang Ren, Will Hamilton, and Jure Leskovec. Hier-
815 archical graph representation learning with differentiable pooling. *Advances in neural information*
816 *processing systems*, 31, 2018b.
- 817
818 Jianke Yu, Hanchen Wang, Xiaoyang Wang, Zhao Li, Lu Qin, Wenjie Zhang, Jian Liao, and Ying
819 Zhang. Group-based fraud detection network on e-commerce platforms. In *Proceedings of the*
820 *29th ACM SIGKDD Conference on Knowledge Discovery and Data Mining*, pp. 5463–5475,
2023.
- 821
822 Kaiwei Zhang, Junchi Yu, Haichao Shi, Jian Liang, and Xiao-Yu Zhang. Rumor detection with di-
823 verse counterfactual evidence. In *Proceedings of the 29th ACM SIGKDD Conference on Knowl-*
824 *edge Discovery and Data Mining*, pp. 3321–3331, 2023.
- 825
826 Liang Zhang, Xudong Wang, Hongsheng Li, Guangming Zhu, Peiyi Shen, Ping Li, Xiaoyuan Lu,
827 Syed Afaq Ali Shah, and Mohammed Bennamoun. Structure-feature based graph self-adaptive
pooling. In *Proceedings of The Web Conference 2020*, pp. 3098–3104, 2020a.
- 828
829 Yanfu Zhang, Hongchang Gao, Jian Pei, and Heng Huang. Robust self-supervised structural graph
830 neural network for social network prediction. In *Proceedings of the ACM Web Conference 2022*,
831 pp. 1352–1361, 2022.
- 832
833 Zhen Zhang, Jiajun Bu, Martin Ester, Jianfeng Zhang, Chengwei Yao, Zhi Yu, and Can Wang.
Hierarchical graph pooling with structure learning. *arXiv preprint arXiv:1911.05954*, 2019.
- 834
835 Zhen Zhang, Fan Wu, and Wee Sun Lee. Factor graph neural networks. *Advances in Neural Infor-*
836 *mation Processing Systems*, 33:8577–8587, 2020b.
- 837
838 Zhen Zhang, Jiajun Bu, Martin Ester, Jianfeng Zhang, Zhao Li, Chengwei Yao, Huifen Dai, Zhi Yu,
839 and Can Wang. Hierarchical multi-view graph pooling with structure learning. *IEEE Transactions*
on Knowledge and Data Engineering, 35(1):545–559, 2021.
- 840
841 Xiaowei Zhou, Jie Yin, and Ivor W Tsang. Edge but not least: Cross-view graph pooling. In
842 *Joint European Conference on Machine Learning and Knowledge Discovery in Databases*, pp.
344–359. Springer, 2022.
- 843
844
845
846
847
848
849
850
851
852
853
854
855
856
857
858
859
860
861
862
863

APPENDIX

A RELATED WORK

A.1 GRAPH CLASSIFICATION AND GRAPH REGRESSION

Graphs provide an effective tool to represent interaction among different objects (Wu et al., 2020b). Graph classification (Baek et al., 2021) is a fundamental graph machine learning problem, which aims to classify each graph into its corresponding category. The majority of current works adopt message passing mechanisms (Wu et al., 2020b), where each node receives information from its neighbors in a recursive manner. Then, a graph readout function is adopted to summarize all node representations into a graph-level representation for downstream classification. Graph classification has extensive applications in various domains such as molecular property prediction (Wieder et al., 2020) and protein function analysis (Mills et al., 2018). Graph regression (Qin et al., 2023) is close to graph classification which maps graph-level data into continuous vectors. Researchers usually utilize graph regression to formulate molecular property predictions (Mqawass & Popov, 2024). Graph pooling has been an important topic in graph-level tasks (Knyazev et al., 2019; Lee et al., 2019; Ranjan et al., 2020; Ma et al., 2020b; Zhou et al., 2022; Pang et al., 2021; Bacciu et al., 2023; Zhang et al., 2020a; 2019; Hansen & Bianchi, 2023; Ying et al., 2018a; Bianchi et al., 2020; Tsitsulin et al., 2023a; Duval & Malliaros, 2022; Bianchi, 2022), which generally utilize a hierarchical way to refine the graph structures (Bianchi & Lachi, 2024; Liu et al., 2022b). In this work, we generally study the performance of graph pooling on graph-level tasks and validate the effectiveness of graph pooling approaches in most cases.

A.2 NODE CLASSIFICATION

Node classification aims to classify each node in a graph based on its attributes and relationship with the other nodes (Xiao et al., 2022; Ju et al., 2024). Node classification has various applications in the real world, including social network analysis (Camacho et al., 2020), knowledge graphs (Ye et al., 2022), bioinformatics (Bhagat et al., 2011) and online commerce services (Yu et al., 2023). Graph neural networks have been widely utilized to solve the problem by learning semantics information across nodes by neighborhood propagation. Since graph pooling would reduce the number of nodes, recent works utilize a U-Net architecture (Gao & Ji, 2019), which involves down-sampling and up-sampling with residue connections. In this work, we systematically evaluate the performance of graph pooling on node classification and observe that graph pooling has limited improvement compared with basic graph neural network architectures.

A.3 PREVIOUS BENCHMARK RESEARCH

Previous studies have built benchmark for graph-related tasks (Errica et al., 2019; Hu et al., 2020b). In particular, Errica et al. (2019) is a benchmark including six different GNN models across nine commonly used TUDataset datasets. Open Graph Benchmark (OGB) (Hu et al., 2020b) evaluate different graph neural network approaches experiments on graph classification, graph regression, and node classification. Errica et al. (2019) only involve one graph pooling method and Hu et al. (2020b) does not involve any graph pooling methods. In comparison, our method focuses on graph pooling techniques rather than graph neural networks. Moreover, our benchmark explores the robustness of these methods by introducing noise attacks in both graph classification and node classification tasks and investigate their generalizability through out-of-distribution shifts.

B DETAILS OF U-NET BASED NODE CLASSIFICATION

Most existing studies that combine node classification with pooling have utilized the U-Net architecture (Wu et al., 2022a; Song et al., 2024; Zhang et al., 2021). Figure A.1 shows the overview of the U-Net framework. Pooling plays a crucial role in the U-Net structure, as it progressively reduces the graph size in the downsampling path to extract important global features while preserving essential local information. In the upsampling path, pooling facilitates the fusion of features from the downsampling path with those being progressively recovered in the upsampling path through

918
919
920
921
922
923
924
925
926
927
928
929
930
931
932
933
934
935
936
937
938
939
940
941
942
943
944
945
946
947
948
949
950
951
952
953
954
955
956
957
958
959
960
961
962
963
964
965
966
967
968
969
970
971

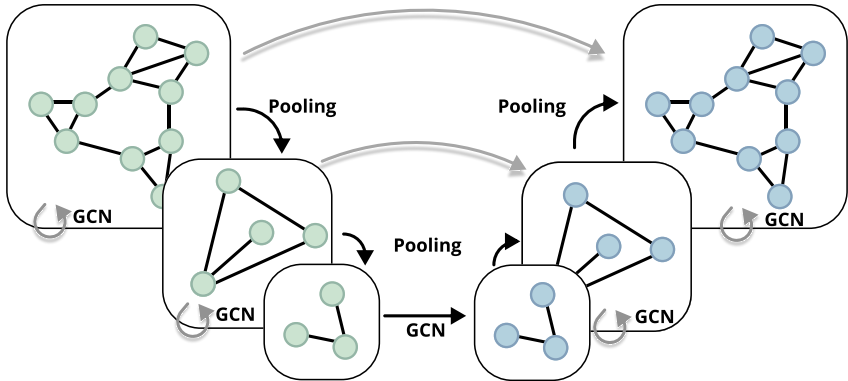


Figure A.1: Overview of the graph U-Net framework for node classification.

skip connections, thereby assisting the model in accurately performing graph node classification or other tasks. Pooling not only simplifies the graph’s complexity but also provides the model with multi-scale feature representation capabilities.

In the downsampling path, the input feature matrix is first subjected to graph convolution, where the product of the adjacency matrix and the feature matrix, along with the weighted sum of the weight matrix and the bias term, yields the activated feature matrix $\mathbf{H}^{(l+1)}$. Next, a pooling operation is applied, reducing the number of nodes by selecting those with higher scores, thereby transforming the original feature matrix ($\mathbf{H}^{(l+1)}$) and adjacency matrix $\mathbf{A}^{(l)}$ into a smaller feature matrix $\mathbf{H}'^{(l+1)}$ and a corresponding adjacency matrix $\mathbf{A}'^{(l+1)}$. In the upsampling path, the pooled feature matrix $\mathbf{H}'^{(l+1)}$ is first upsampled to restore the original number of nodes, generating a new feature matrix $\mathbf{H}''^{(l+1)}$. Then, the restored feature matrix is concatenated with the corresponding feature matrix $\mathbf{H}^{(l)}$ from the downsampling path, forming the merged feature matrix $\mathbf{H}_{\text{merged}}^{(l+1)}$. Finally, the merged feature matrix undergoes another graph convolution, resulting in the output feature matrix $\mathbf{H}^{(l+2)}$.

C DETAILS OF SELECTED POOLING METHODS

C.1 NODE DROPPING POOLING

TopKPool (Knyazev et al., 2019). TopKPool utilizes the attention mechanism to learn the scores of different nodes and then selects the nodes with top scores, which can learn important local portions from original graphs.

SAGPool (Lee et al., 2019). SAGPool utilizes a different graph neural network to learn importance scores, which can guide the pooling process effectively.

ASAPool (Ranjan et al., 2020). ASAPool considers the neighboring subgraphs to represent nodes and then adopts the attention mechanism to generate subgraph representations. The importance nodes are selected by a graph neural networks with local extremum information.

PANPool (Ma et al., 2020b). PANPool constructs the maximal entropy transition (MET) matrix based on graph Laplacian, which can generate importance scores for different nodes.

COPool (Zhou et al., 2022). COPool learns pooled representations from the complimentary edge and node views. The edge view comes from high-order semantics information while the node view stems from importance scores from the cut proximity matrix.

CGIPool (Pang et al., 2021). CGIPool incorporates mutual information optimization into graph pooling, which can enhance the graph-level relationships between the original graph and the pooled graph.

KMISPool (Bacciu et al., 2023). KMISPool incorporates the Maximal k-Independent Sets (k-MIS) into graph pooling, which can detect the important nodes in the graph with topological preserved.

GSAPool (Zhang et al., 2020a). GSAPool integrates both structural and attribute information in different components. These scores from different components are then fused to guide the graph pooling process.

HGPSLPool (Zhang et al., 2019). HGPSLPool not only utilizes graph pooling to determine important nodes from the original graph, but also leverages graph structure learning to explore the topological information in the pooled graph.

C.2 NODE CLUSTERING POOLING

AsymCheegerCutPool (Hansen & Bianchi, 2023). AsymCheegerCutPool conducts graph clustering to generate the assignment of each node according to graph total variation (GTV). Each cluster is aggregated in a hierarchical manner during graph pooling.

DiffPool (Ying et al., 2018a). DiffPool introduces a learnable soft assignment of each node during graph clustering, and then maps each cluster into the coarsened nodes in the pooling graph.

MincutPool (Bianchi et al., 2020). MincutPool relaxes the classic normalized mincut problem into a continuous fashion, and then optimizes a graph neural network to achieve this. The graph clustering results are adopted to guide the graph pooling process.

DMoNPool (Tsitsulin et al., 2023a). DMoNPool introduces an objective based on modularity for graph clustering and then adds a regularization term to avoid trivial solutions during optimization. Similarly, graph clustering results are leveraged for graph pooling.

HoscPool (Duval & Malliaros, 2022). HoscPool combines higher-order relationships in the graph with graph pooling based on motif conductance. It minimizes a relaxed motif spectral clustering objective and involves multiple motifs to learn hierarchical semantics.

JustBalancePool (Bianchi, 2022). JustBalancePool consists of two components. On the one hand, it aims to reduce the local quadratic variation during graph clustering. On the other hand, it involves a balanced term to reduce the risk of degenerate solutions.

SEPool (Wu et al., 2022a). SEPool generates a clustering assignment matrix in one go through a global optimization algorithm, avoiding the suboptimality associated with layer-by-layer pooling.

ParsPool (Song et al., 2024). ParsPool is characterized by the introduction of a graph parsing algorithm that adaptively learns a personalized pooling structure for each graph. ParsPool is inspired by bottom-up grammar induction and can generate a flexible pooling tree structure for each graph.

D DETAILED DESCRIPTION OF DATASETS

D.1 GRAPH CLASSIFICATION

Table A.1 provides descriptive statistics of the selected datasets, revealing that our chosen datasets encompass graph data of varying scales and features. This diversity establishes a robust foundation for benchmarking. The following are detailed descriptions of these datasets:

Ogbg-molpcba comprises a collection of 437,929 molecules, each represented as a graph where nodes are atoms and edges indicate chemical bonds between atoms. Each node is associated with features such as atom type, valence, and charge. The dataset involves 128 biological activity labels, each representing a binary classification task that indicates whether a molecule exhibits a specific biological activity (Hu et al., 2020b).

PROTEINS represents protein structures; nodes denote secondary structure elements (SSEs) and the edges indicate the relationships between these SSEs that are in close proximity. The primary goal of this dataset is to assist in the classification of proteins into different structural classes based on their amino acid sequences and structure— structural characteristics. Each graph’s label is the protein class, so the dataset covers diverse protein structures (Borgwardt et al., 2005).

PROTEINS_FULL is an extended version of PROTEINS. Each graph directly represents a protein structure: nodes correspond to SSEs like alpha helices and beta sheets (Borgwardt et al., 2005).

NCI1 is a collection of chemical compound graphs. Originating from the National Cancer Institute (NCI) database, each graph sample is a compound in which nodes represent atoms and edges represent the bonds between them. The dataset is binary-class labeled, indicating biological activity via compounds' anti-cancer activity against specific cell lines (Wale et al., 2008).

NCI109 is also a collection of chemical compound graphs derived from NCI. Similarly, each node in the graph denotes an atom and each edge denotes a bond. The two classes in NCI109 are about compounds' ability to inhibit or interact with the specified cancer cell line (Wale et al., 2008).

MUTAG consists of 188 chemical molecule graphs, where each node represents an atom. The nodes have different atomic types, such as carbon, nitrogen, oxygen, etc. Edges represent chemical bonds between atoms, such as single or double bonds, indicating their connections in the molecule. The objective is to predict whether each molecule is mutagenic, with positive labels indicating mutagenic molecules and negative labels indicating non-mutagenic molecules (Morris et al., 2020).

D&D is a dataset of protein structure graphs for graph classification. Each graph in this dataset represents a protein, with nodes corresponding to amino acids and edges corresponding to the spatial or sequential proximity between these amino acids. The primary objective of the D&D dataset is to classify proteins into one of two categories: enzymes or non-enzymes (Shervashidze et al., 2011).

IMDB-B is a collection of social network graphs derived from the Internet Movie Database (IMDB). Each graph is about a collaboration network from movies whereby nodes stand for actors or actresses and edges indicate that the two actors appeared in the same movie — this dataset comprises two classes reflecting the movie genres (Cai & Wang, 2018).

IMDB-M, similar to IMDB-B, represents each movie as a graph where the nodes represent actors and the edges represent co-appearances of actors in the same movie. However, the nodes in IMDB-M are categorized into three classes, and it includes a larger number of actors (Cai & Wang, 2018).

COLLAB consists of 5,000 graphs, each representing a collaboration network of a group of authors in different research fields. In each graph, nodes represent authors, and edges represent collaborations between authors, indicating that the connected authors have co-authored at least one paper. The graphs have three classes, each corresponding to an academic research field. (Morris et al., 2020).

COX2 consists of 467 graphs, where each graph corresponds to a molecule. The nodes represent atoms, and the edges represent chemical bonds, and the graph label indicates whether the molecule is a COX-2 inhibitor (Sutherland et al., 2003).

AIDS consists of 2,000 graphs. Each graph corresponds to a molecule, where the nodes represent individual atoms and the edges represent chemical bonds between these atoms. The goal is to predict the inhibitory effect of molecules on HIV based on their structure. (Riesen & Bunke, 2008).

FRANKENSTEIN consists of 4,337 graphs. Each graph in this dataset represents a chemical compound, where the nodes correspond to atoms, and the edges represent the bonds between them. The graph labels indicate whether the molecule is considered an active compound (Orsini et al., 2015).

Mutagenicity contains 4,337 molecular graphs. In Mutagenicity, each graph represents a molecule, where the nodes are atoms and the edges denote chemical bonds between the nodes. The classification goal is to predict whether a molecule is mutagenic or not (Debnath et al., 1991).

D.2 GRAPH REGRESSION

Table A.2 provides an overview of the selected datasets in terms of their tasks, compounds and their features, recommended splits, and metrics. A more detailed description is provided below.

QM7 and QM8 are benchmark datasets in computational chemistry, designed to facilitate the development and evaluation of machine learning approaches for quantum mechanical property prediction. It contains approximately 7,165 (QM7) and 21,786 (QM8) molecular structures, each characterized by their calculated properties using quantum chemistry methods, specifically focusing on electronic spectra (Wu et al., 2018; Montavon et al., 2013).

BACE is a collection of biochemical data used to evaluate computational methods for drug discovery. The dataset includes a total of 1,522 compounds, each annotated with their binding affinities,

Table A.1: Summary statistics of datasets for **graph classification**. CC denotes the clustering coefficient, and Diameter representing the maximum value of the shortest path between any two nodes in the graph.

Datasets	Graphs	Classes	Avg. Nodes	Avg. Edges	Node Attr.	Avg. Diameter	Avg. Degree	Avg. CC
Ogbg-molpcba	437,929	2*128	26.00	27.50	-	12.00	2.20	0.00
PROTEINS	1,113	2	39.06	72.82	+ (1)	11.14	3.73	0.51
PROTEINS_full	1,113	2	39.06	72.82	+ (29)	11.14	3.73	0.51
NCII	4,110	2	29.87	32.30	-	11.45	2.16	0.00
NCII09	4,127	2	29.68	32.13	-	11.21	2.16	0.00
MUTAG	188	2	17.90	39.60	+ (7)	8.22	2.19	0.00
D&D	1,178	2	284.32	715.66	-	16.45	4.92	0.48
IMDB-B	1,000	2	19.77	96.53	-	1.86	8.89	0.95
IMDB-M	1,500	3	13.00	65.94	-	1.47	8.10	0.97
COLLAB	5,000	3	74.49	2457.22	-	1.86	37.36	0.89
COX2	467	2	41.22	43.45	+ (3)	13.79	2.11	0.00
AIDS	2,000	2	15.69	16.20	+ (4)	6.56	2.01	0.01
FRANKENSTEIN	4,337	2	16.90	17.88	+ (780)	7.86	2.06	0.01
Mutagenicity	4,337	2	30.32	30.77	-	9.10	2.04	0.00

Table A.2: Details of datasets for **graph regression**.

Datasets	Tasks	Compounds	Split	Avg. Nodes	Avg. Edges	Avg. Diameter	Avg. Degree	Avg. CC
QM7	1	7,165	Scaffold	6.79	6.44	4.21	1.89	0.06
QM8	12	21,786	Random	7.77	8.09	4.35	2.08	0.09
BACE	1	1,522	Scaffold	34.09	36.86	4.35	2.08	0.01
ESOL	1	1,128	Random	13.30	13.69	7.02	1.98	0.00
FreeSolv	1	643	Random	8.76	8.43	5.06	1.84	0.00
Lipophilicity	1	4,200	Random	27.04	29.50	13.85	2.18	0.00

as well as molecular descriptors and fingerprints to facilitate the development and assessment of machine learning models (Wu et al., 2018; Ciordia et al., 2016).

ESOL is a prominent resource in cheminformatics, designed for evaluating machine learning models on the prediction of aqueous solubility of small molecules. The dataset, derived from the work of Delaney, encompasses a diverse range of chemical compounds with experimentally determined solubility values expressed in logS, where S is the solubility in mols per liter. It includes 1128 compounds, serving as a benchmark for solubility prediction tasks (Delaney, 2004; Wu et al., 2018).

FreeSolv is a dataset containing hydration-free energies for small molecules in an aqueous solution. It comprises data for a wide range of organic molecules, providing both experimental values and calculated predictions based on molecular simulations (Mobley & Guthrie, 2014; Wu et al., 2018).

Lipophilicity is primarily utilized for studying and evaluating molecular lipophilicity. This dataset comprises 4,200 compounds sourced from the ChEMBL database, with experimentally measured partition coefficient (logD) values that reflect the distribution behavior of compounds in a water-octanol system (Lukashina et al., 2020; Wu et al., 2018).

D.3 NODE CLASSIFICATION

Table A.3 presents descriptive statistics of the seven datasets used for node classification. It is evident that there is a significant variance in the scale of the selected datasets, each possessing distinct characteristics. Further background information and details about these datasets are provided below.

Ogbn-arxiv comprises a collection of 169,343 scientific publications classified into 40 distinct categories. Each paper is represented by a node with a 128-dimensional feature, which comes from the average of word embeddings in the corresponding title and abstract. Edges indicate citation relationships between papers (Hu et al., 2020b).

Cora comprises a collection of 2,708 scientific publications classified into seven distinct categories. Each publication in the dataset is represented as a node in a citation network, where edges indicate citation relationships between papers (Yang et al., 2016).

Table A.3: Summary statistics of datasets for **node classification**.

Datasets	Number of Nodes	Number of Edges	Number of Features	Number of Classes	Diameter	Avg. Degree	Avg. CC
Ogbn-arxiv	169,343	1,166,243	128	40	23	13.72	0.23
Cora	2,708	10,556	1,433	7	NA	3.90	0.24
CiteSeer	3,327	9,104	3,703	6	NA	2.74	0.14
PubMed	19,717	88,648	500	3	18	4.50	0.06
Cornell	183	298	1,703	5	8	3.06	0.17
Texas	183	325	1,703	5	8	3.22	0.20
Wisconsin	251	515	1,703	5	8	3.71	0.21
Github	37,700	578,006	0	2	7	15.33	0.01

CiteSeer is a widely used citation network dataset. It comprises scientific publications categorized into six classes, with each publication represented by a 3,327-dimensional binary vector recording the presence or absence of specific words (Yang et al., 2016).

PubMed consists of scientific publications from the PubMed database, categorized into three classes based on their Medical Subject Headings (MeSH) terms. Each node has a sparse bag-of-words vector derived from the content of the corresponding publication (Yang et al., 2016).

Cornell, Texas, and Wisconsin are made up of nodes that represent web pages and edges which denote hyperlinks between these pages. Each node has a class which denotes the topic of the web page; this allows tasks including node classification and link prediction to be performed. The datasets differ in size: Cornell and Texas each have 183 nodes while Wisconsin has 251 nodes (Pei et al., 2020).

Github includes node attributes representing the features of developers, such as their interests, skills, and contributions to various repositories. The edges within the network capture the interactions and collaborations of developers, creating a multi-faceted graph structure (Rozemberczki et al., 2021).

D.4 OUT-OF-DISTRIBUTION SHIFTS

Size shifts. For the selected datasets, including NCI1, D&D, NCI109, and IMDB-B, we utilized the data provided by the authors of size-invariant-GNNs (Bevilacqua et al., 2021). In this setup, the graphs with the smallest 50% of nodes are used as the training set, those with the largest 20% of nodes are used as the test set, and the remaining graphs were used as the validation set. The data can be downloaded from <https://www.dropbox.com/s/38eg3twe4dd1hbt/data.zip>.

Density shifts. For the selected datasets, we divide the datasets based on graph density: the 50% of graphs with the lowest density are used as the training set, the 20% with the highest density are used as the test set, and the remaining graphs are used as the validation set. After applying density shifts, the following densities are observed: for D&D, the training set density is 0.0274, the validation set density is 0.0536, the test set density is 0.1142; for NCI1, the training set density is 0.1229, the validation set density is 0.1920, the test set density is 0.2786; for NCI109, the training set density is 0.1248, the validation set density is 0.1943, the test set density is 0.2770; for IMDB-B, the training set density is 0.6574, the validation set density is 1.1074, the test set density is 1.7427.

Degree shifts. For the selected datasets, we divide the datasets based on node degree: the 50% of nodes with the highest degree are used as the training set, the 25% with the lowest degree are used as the test set, and the remaining nodes are used as the validation set. After applying degree shifts, we can observe that: for Cora, the training set average degree is 5.9431, the validation set average degree is 2.4225, and the test set average degree is 1.2836; for Citeseer, the training set average degree is 4.3313, the validation set average degree is 1.3430, and the test set average degree is 0.9424; for Pubmed, the training set average degree is 7.9148, the validation set average degree is 1.1552, and the test set average degree is 1.0000; for Cornell, the training set average degree is 3.2198, the validation set average degree is 0.1111, and the test set average degree is 0.0000; for Texas, the training set average degree is 3.3626, the validation set average degree is 0.4222, and the test set average degree is 0.0000; for Wisconsin, the training set average degree is 3.7600, the validation set average degree is 0.7258, and the test set average degree is 0.0000.

Closeness shifts. For the selected datasets, we divide the datasets based on node closeness: the 50% of nodes with the lowest closeness are used as the training set, the 25% with the highest closeness are used as the test set, the remaining nodes used as the validation set. After applying closeness shifts, we can observe that: for Cora, the training set average closeness is 0.1076, the validation set average

Table A.4: Details of hyperparameter tuning for different pooling methods

Methods		Hyperparameter space
<i>Node Dropping Pooling</i>		
TopKPool	NIPS'19	Pooling ratio: 0.1, 0.3, 0.5, 0.7, 0.9
SAGPool	ICML'19	Pooling ratio: 0.1, 0.3, 0.5, 0.7, 0.9
ASAPool	AAAI'20	Pooling ratio: 0.1, 0.3, 0.5, 0.7, 0.9
PANPool	NIPS'20	Pooling ratio: 0.1, 0.3, 0.5, 0.7, 0.9
COPool	ECMLPKDD'22	Pooling ratio: 0.1, 0.3, 0.5, 0.7, 0.9; K: 1, 2, 3
CGIPool	SIGIR'22	Pooling ratio: 0.1, 0.3, 0.5, 0.7, 0.9
KMISPool	AAAI'23	The independent sets K : 1, 2, 3, 4, 5
GSAPool	WWW'20	Pooling ratio: 0.1, 0.3, 0.5, 0.7, 0.9; Alpha: 0.2, 0.4, 0.6, 0.8
HGPSLPool	Arxiv'19	Pooling ratio: 0.1, 0.3, 0.5, 0.7, 0.9
ParsPool	ICLR'24	Parsingnet layers: 1, 2, 3; Deepsets layers: 1, 2, 3
<i>Node Clustering Pooling</i>		
AsymCheegerCutPool	ICML'23	MLP layers: 1, 2; MLP hidden channels: 64, 128, 256
DiffPool	NIPS'18	Not applicable
MincutPool	ICML'20	Temperature: 1, 1.5, 1.8, 2.0
DMoNPool	JMLR'23	Clusters: 2, 4, 6, 8, 10, 12
HoscPool	CIKM'22	Mu: 0.2, 0.5, 0.8; Alpha: 0.2, 0.5, 0.8
JustBalancePool	Arxiv'22	Not applicable
SEPool	ICML'22	Tree depth: 1, 2, 3; Number of blocks: 1, 2, 3, 4

closeness is 0.1560, the test set average closeness is 0.1786; for Citeseer, the training set average closeness is 0.0150, the validation set average closeness is 0.0679, the test set average closeness is 0.0832; for Pubmed, the training set average closeness is 0.1448, the validation set average closeness is 0.1669, the test set average closeness is 0.1850; for Cornell, the training set average closeness is 0.2690, the validation set average closeness is 0.3754, the test set average closeness is 0.3896; for Texas, the training set average closeness is 0.2899, the validation set average closeness is 0.3887, the test set average closeness is 0.4047; for Wisconsin, the training set average closeness is 0.2630, the validation set average closeness is 0.3686, the test set average closeness is 0.3855.

E ADDITIONAL EXPERIMENTAL DETAILS

E.1 GRAPH CLASSIFICATION

The classification model comprises three primary components: GCNConv layers, pooling methods, and a global average pooling layer. The hidden and output channels for this model are both set to 64. Initially, the data passes through three GCNConv layers with ReLU activation functions, followed by two pooling layers, before arriving at a global average pooling layer. The embedding output from this global layer undergoes further processing through a linear layer with ReLU activation, having dimensions (64, 32), followed by another linear layer without any activation function but with dimensions (32, number of classes). The final output can be available after applying softmax to the embedding output. All models use the Adam optimizer with a learning rate of 0.001 and are trained for 200 epochs by minimizing the negative log-likelihood loss function. For Ogbg-molpcba, the data is divided into training, validation, and test sets with an 80%, 10%, and 10% split, respectively. The remaining datasets are divided into training, validation, and test sets with a 70%, 15%, and 15% split. Each trial is repeated multiple times with different random seeds.

E.2 GRAPH REGRESSION

We use a backbone network inspired by MESPool (Xu et al., 2024a) for graph regression. The model mainly consists of three GINConv layers with ReLU activation functions and BatchNorm, along with two pooling layers, followed by a global average pooling layer. All channels (both hidden and output) are set to 64. The embedding output from the global average pooling layer passes through another linear layer with ReLU activation, having dimensions (64, 32). All models use the Adam optimizer with a learning rate of 0.001 and are trained for 200 epochs by minimizing the negative

1242 log-likelihood loss function. All data are processed using a 5-fold cross-validation and are run on
1243 multiple different seeds.

1244 E.3 NODE CLASSIFICATION

1245 For node classification, we utilize a U-Net architecture, which we divide into a downsampling con-
1246 volutional part and an upsampling convolutional part (Siddique et al., 2021). The downsampling
1247 convolutional section includes two GCNConv layers with ReLU activation functions, with pooling
1248 applied between these layers. In the upsampling convolutional section, we use the indices saved
1249 during pooling for upsampling, restoring features to their pre-pooling size. The upsampled features
1250 are then fused with the corresponding residual features from the downsampling path, either through
1251 summation or concatenation. Finally, the fused features are processed and activated through a GCN-
1252 Conv layer. All models employ the Adam optimizer with a learning rate set to 0.001 and are trained
1253 for 200 epochs using cross-entropy loss. All data are processed using a 5-fold cross-validation and
1254 are run on multiple different seeds.

1255 E.4 HYPERPARAMETER TUNING

1256 Details of hyperparameter tuning for different pooling methods can be found in Table A.4. We
1257 performed hyperparameter searches for each dataset in each task.

1258 F ADDITIONAL EXPERIMENTS

1259 F.1 ROBUSTNESS ANALYSIS

1260 Table A.5 shows the additional robustness analysis on more node-level datasets. From Table A.5,
1261 we observe the following: Firstly, for smaller node classification datasets such as Cornell, Texas,
1262 and Wisconsin, masking node features results in the greatest performance loss, while edge deletion
1263 leads to the smallest performance loss. The potential reason is that these smaller datasets inherently
1264 possess higher local characteristics and structural sparsity, making node features more critical for the
1265 model’s classification tasks. Secondly, consistent with the robustness analysis on Cora, Citeseer, and
1266 Pubmed, ASAPool and KMISPool demonstrate superior performance, indicating that these pooling
1267 methods exhibit stronger robustness in node classification tasks.

1268 F.2 GENERALIZABILITY ANALYSIS

1269 Table A.6 presents the results of size-based and density-based distribution shifts on NCI109 and
1270 IMDB-B, respectively. From Table A.6, we obtain conclusions similar to those in the main text: for
1271 the NCI109 dataset, node dropping pooling methods perform worse than node clustering pooling
1272 methods, whereas on the IMDB-B dataset, node dropping pooling methods outperform node clus-
1273 tering pooling methods. Overall, AsymCheegerCutPool, MinCutPool, and DMonPool outperform
1274 other pooling methods.

1275 Table A.7 presents the results of degree-based and closeness-based distribution shifts on node clas-
1276 sification tasks across four datasets: Pubmed, Cornell, Texas, and Wisconsin. We observe the fol-
1277 lowing: *Firstly*, KMISPool and GSAPool generally perform the best, yet no single pooling method
1278 consistently leads across all datasets. *Secondly*, the issue of class imbalance persists, and it is more
1279 pronounced in smaller datasets such as Cornell, Texas, and Wisconsin. *Thirdly*, smaller datasets like
1280 Cornell, Texas, and Wisconsin are more sensitive to distribution shifts compared to the larger dataset
1281 Pubmed, resulting in more significant performance degradation.

Table A.5: Results of node classification under random noise attack.

Dataset	Ptb Method	TopKPool	SAGPool	ASAPool	PANPool	COPool	CGIPool	KMISPool	GSAPool	HGPSLPool
Cornell	ADD	46.64±0.25	46.45±0.77	47.18±1.03	47.00±1.18	46.63±0.25	46.63±0.92	46.81±0.67	46.81±1.12	46.45±0.45
	DROP	61.73±1.17	62.09±1.84	62.29±1.15	61.93±0.95	62.25±0.44	61.36±2.00	63.19±1.79	63.01±0.54	62.46±1.33
	MASK	46.99±0.90	47.36±1.56	47.91±2.46	47.00±0.45	48.11±1.17	46.63±1.03	47.74±1.13	47.01±1.35	47.55±1.19
Texas	ADD	58.63±0.67	61.37±0.94	60.48±0.62	59.92±0.92	59.01±0.44	58.99±1.14	58.83±0.49	59.37±1.39	58.63±0.23
	DROP	64.47±2.02	64.47±0.42	63.92±2.38	64.30±0.89	63.92±1.96	63.57±1.40	65.57±1.59	65.57±1.33	63.57±2.06
	MASK	57.56±0.92	57.93±1.55	58.85±1.44	57.19±0.91	57.37±1.33	57.56±0.93	<u>58.10±1.09</u>	57.93±0.92	57.92±0.43
Wisconsin	ADD	54.46±0.99	53.66±0.98	56.18±1.49	55.52±0.21	55.78±0.98	55.78±1.30	54.99±0.34	54.73±0.48	53.65±0.37
	DROP	<u>61.23±1.23</u>	60.55±1.15	60.29±1.68	59.76±1.72	60.43±1.79	59.36±0.87	60.16±0.66	60.43±0.95	61.36±1.17
	MASK	47.02±0.55	47.94±0.18	<u>49.80±0.86</u>	48.60±1.14	52.59±0.01	48.35±0.49	49.53±1.15	48.20±1.11	48.08±0.96

Table A.6: Results of graph classification under distribution shifts.

Method	NCI109				IMDB-B			
	Size		Density		Size		Density	
	Micro-F1	Macro-F1	Micro-F1	Macro-F1	Micro-F1	Macro-F1	Micro-F1	Macro-F1
<i>Node Dropping Pooling</i>								
TopKPool	25.10±0.81	22.90±1.01	55.92±2.57	54.88±1.42	56.00±1.22	53.34±2.26	72.00±5.94	68.13±5.78
SAGPool	24.07±1.29	21.64±1.58	53.31±1.74	51.46±0.98	67.67±5.10	67.44±4.97	74.27±3.92	67.13±5.78
ASAPool	22.57±0.70	19.42±1.04	58.42±2.73	57.09±2.02	73.83±12.43	73.70±12.36	80.80±4.94	78.70±4.15
PANPool	25.73±0.11	23.80±0.12	56.25±1.63	54.34±1.93	66.50±9.34	65.73±10.38	76.27±4.21	71.65±4.67
COPool	24.94±1.72	22.77±2.31	57.10±2.20	55.39±1.21	65.33±2.72	65.13±2.94	72.40±9.91	69.52±8.26
CGIPool	24.54±1.19	22.39±1.46	61.36±0.84	57.98±3.78	72.83±8.00	72.69±7.87	71.60±5.44	63.60±7.27
KMISPool	43.78±5.82	43.24±5.33	58.08±3.45	50.03±6.64	75.33±4.78	75.16±4.61	78.80±0.86	73.74±0.63
GSAPool	25.97±3.11	24.00±4.03	53.04±1.30	52.64±1.16	70.17±3.70	69.17±4.45	78.80±0.86	73.11±0.99
HGPSLPool	21.54±0.22	18.17±0.43	58.18±2.26	55.06±3.02	69.33±4.71	69.25±4.76	75.07±1.86	70.37±1.81
ParsPool	42.68±0.81	41.97±0.74	59.91±1.13	56.13±2.70	<u>75.00±3.63</u>	<u>74.92±3.57</u>	76.00±2.99	71.63±3.00
<i>Node Clustering Pooling</i>								
AsymCheegerCutPool	79.18±0.00	49.92±0.12	68.53±0.00	44.29±0.00	71.50±0.60	71.45±0.60	78.80±0.00	73.75±0.00
DiffPool	21.38±0.00	17.61±0.00	69.47±0.00	48.65±0.02	69.17±0.70	67.31±0.83	65.20±1.10	62.72±0.76
MinCutPool	31.83±0.77	30.50±0.90	70.76±0.00	56.27±0.02	70.17±0.01	68.28±0.03	78.40±0.01	73.91±0.02
DMoNPool	79.41±0.01	55.84±0.01	67.44±0.05	55.80±0.13	74.33±1.59	73.85±1.61	77.33±0.13	72.56±0.20
HoscPool	33.73±2.35	30.58±2.13	69.54±0.05	54.41±0.03	72.83±0.09	72.37±0.10	77.20±0.04	73.43±0.05
JustBalancePool	58.43±4.14	44.15±1.17	71.26±0.00	58.08±0.01	76.17±0.17	74.69±0.35	78.40±0.01	73.91±0.02

Table A.7: Results of node classification under distribution shifts.

Method	Pubmed				Cornell			
	Degree		Closeness		Degree		Closeness	
	Micro-F1	Macro-F1	Micro-F1	Macro-F1	Micro-F1	Macro-F1	Micro-F1	Macro-F1
TopKPool	81.66±0.32	81.11±0.38	85.66±0.09	82.36±0.24	34.07±2.10	22.35±2.92	57.78±4.80	25.56±8.37
SAGPool	83.07±1.02	82.57±1.07	85.96±0.34	82.73±0.38	36.30±4.19	<u>24.39±4.03</u>	61.48±4.57	31.54±8.24
ASAPool	82.11±0.12	81.94±0.55	85.02±0.54	82.12±0.77	34.07±1.05	20.94±3.40	60.74±2.77	26.33±2.21
PANPool	81.65±0.12	81.15±0.11	85.55±0.03	82.16±0.20	<u>35.56±0.00</u>	23.55±0.90	54.07±2.10	18.58±3.28
COPool	80.42±0.14	79.82±0.20	84.99±0.35	81.81±0.29	35.56±1.81	22.64±3.21	49.63±6.87	21.09±3.44
CGIPool	80.35±1.33	79.69±1.32	84.97±0.75	81.74±0.90	36.30±4.19	25.34±4.15	60.00±1.81	27.48±3.60
KMISPool	83.41±0.02	82.92±0.03	85.66±0.07	82.50±0.12	34.81±1.05	22.99±2.00	58.52±5.54	24.70±8.45
GSAPool	83.15±0.81	<u>82.61±0.83</u>	<u>85.83±0.32</u>	<u>82.70±0.50</u>	35.56±1.81	23.23±1.21	62.22±1.81	<u>30.06±4.20</u>
HGPSLPool	OOM	OOM	OOM	OOM	34.07±1.05	21.39±1.41	57.78±1.81	23.63±1.61
<i>Texas</i>								
<i>Wisconsin</i>								
Method	Degree		Closeness		Degree		Closeness	
	Micro-F1	Macro-F1	Micro-F1	Macro-F1	Micro-F1	Macro-F1	Micro-F1	Macro-F1
TopKPool	40.74±2.10	27.06±2.71	61.48±1.05	19.39±0.07	26.88±1.52	19.88±1.97	17.74±2.28	15.34±1.55
SAGPool	39.26±1.05	23.52±0.35	62.22±1.81	19.44±0.35	27.42±1.32	25.32±0.98	18.28±0.76	14.85±0.25
ASAPool	<u>40.74±2.77</u>	23.87±0.67	62.96±1.05	19.58±0.20	29.03±3.48	20.17±1.42	15.59±2.74	11.63±4.27
PANPool	40.00±3.63	23.64±1.13	63.70±1.05	19.72±0.20	30.11±3.31	<u>22.99±1.60</u>	<u>23.66±10.56</u>	15.42±5.61
COPool	39.26±1.05	23.44±0.32	63.70±2.10	19.72±0.39	28.49±1.52	19.94±1.50	16.13±3.95	16.68±3.84
CGIPool	40.00±1.81	23.85±0.52	60.74±1.05	19.25±0.18	25.27±2.74	20.01±2.23	27.96±19.01	20.37±11.58
KMISPool	38.52±1.05	23.19±0.10	63.70±1.05	19.72±0.20	31.72±4.23	22.58±2.76	16.67±0.76	14.20±0.97
GSAPool	40.74±2.10	<u>26.90±2.72</u>	62.22±0.00	19.44±0.00	26.88±3.31	18.51±1.18	15.59±1.52	12.75±1.41
HGPSLPool	<u>40.74±2.77</u>	25.69±3.19	62.96±1.05	19.58±0.20	<u>30.65±1.32</u>	20.76±1.23	16.13±2.63	12.67±1.80